bioRxiv preprint doi: https://doi.org/10.1101/2022.12.29.522099; this version posted December 29, 2022. The copyright holder for this preprint (which was not certified by peer review) is the author/funder, who has granted bioRxiv a license to display the preprint in perpetuity. It is made available under aCC-BY-NC-ND 4.0 International license.

Astroglial mediation of fast-acting antidepressant effect in zebrafish

Marc Duque[1,2,*,†], Alex B. Chen[1,2,3,*,†], Sujatha Narayan[3], David E. Olson[4,5,6,7], Mark C. Fishman[8,‡], Florian Engert[1,‡], Misha B. Ahrens[3,‡]

1 Department of Molecular and Cellular Biology, Harvard University; Cambridge, MA 02138, USA

2 Graduate Program in Neuroscience, Harvard Medical School; Boston, MA 02115, USA

3 Janelia Research Campus, Howard Hughes Medical Institute; Ashburn, VA 20147, USA

4 Department of Chemistry, University of California, Davis; Davis, CA 95616 , USA.

5 Department of Biochemistry and Molecular Medicine, School of Medicine, University of California, Davis; Sacramento, CA 95817, USA.

6 Center for Neuroscience, University of California, Davis; Davis, CA 95618, USA.

7 Institute for Psychedelics and Neurotherapeutics, University of California, Davis, Davis, CA 95616, USA

8 Department of Stem Cell and Regenerative Biology, Harvard University; Cambridge, MA 02138, USA

* mduqueramirez@g.harvard.edu; abchen@g.harvard.edu

†,‡ These authors contributed equally to this work.

Abstract

Rapid-acting antidepressants like ketamine hold promise to change the approach to treatment of major depressive disorder (MDD),[1–3] but their cellular and molecular targets remain unclear. Passivity induced by behavioral futility underlies learned helplessness, a process that becomes maladaptive in MDD.[4,5] Antidepressants inhibit futility-induced passivity (FIP) in rodent models such as the forced swimming[6] or tail suspension[7] tasks, but these models lack the throughput and accessibility for screening compounds and investigating their effects on the brain *in vivo*. Therefore, we adapted a recently discovered FIP behavior[8] in the small and optically accessible larval zebrafish to create a scalable behavioral assay for antidepressant action. We found that rapid-acting antidepressants with diverse pharmacological targets demonstrated a suppression of FIP conserved between fish and rodents. While fast-acting antidepressants are thought to primarily target neurons,[2,9,10] using brain-wide imaging *in vivo* we found, surprisingly, that ketamine, but not psychedelics or typical antidepressants, drove cytosolic calcium elevation in astroglia lasting many minutes. Blocking neural activity did not prevent ketamine's effects on FIP or astroglial calcium, suggesting an astroglia-autonomous mechanism of ketamine's action. Chemogenetic and optogenetic perturbations of astroglia reveal that the aftereffects of calcium elevation are sufficient to suppress FIP by inhibiting astroglial integration of futile swimming. In sum, our work provides evidence that ketamine exerts its antidepressant effects by inhibiting an astroglial population that integrates futility and changes behavioral state. Astroglia play central roles in modulating circuit dynamics,[11] and our work argues that targeting astroglial signaling may be a fruitful strategy for designing new rapid-acting antidepressants.

bioRxiv preprint doi: https://doi.org/10.1101/2022.12.29.522099; this version posted December 29, 2022. The copyright holder for this preprint (which was not certified by peer review) is the author/funder, who has granted bioRxiv a license to display the preprint in perpetuity. It is made available under aCC-BY-NC-ND 4.0 International license.

Main Text

Background

Major depressive disorder (MDD) is a debilitating and widespread condition that is among the most prevalent causes of disability and one of the largest burdens on public health worldwide.[12,13] Moreover, the prevalence of MDD has seen a significant increase across the world due to the COVID-19 pandemic.[14] Therefore, understanding the mechanisms underlying MDD and finding effective treatments is of significant interest to public health. Current pharmacological treatments for MDD are believed to target monoaminergic systems, primarily through blockade of serotonin and/or norepinephrine reuptake in neurons.[15] These agents have many side effects, take weeks to begin alleviating symptoms, and fail to have any therapeutic benefit in $\sim$ 30% of cases.[15] Recently the field has changed dramatically with the advent of fast-acting antidepressant compounds such as ketamine[1,2] and psilocybin.[3] These compounds relieve symptoms in many patients with MDD resistant to conventional treatments, but their use is complicated by their hallucinogenic side-effects and a potential for abuse.[16] A better understanding of fast antidepressants' mechanism of action may shed light on MDD and is essential for generating new therapeutics with safer profiles.

When an individual's attempts to escape an aversive situation are met with futility, the individual will discount the efficacy or value of active struggle and become passive.[4,8,17,18] While futility-induced passivity is ordinarily adaptive in preventing fruitless energy expenditure, maladaptive passivity in response to behavioral futility manifests as learned helplessness[5] or hopelessness, a key clinical criterion for MDD.[19] Futility-induced passivity forms the basis for standard preclinical models of antidepressant activity in rodents, such as the forced swimming,[6] and the tail suspension[7] tests (FST/TST). The prevailing view is that classical and fast-acting antidepressants decrease futility-induced passivity primarily through their actions on neurons, and more specifically by affecting activity in circuits such as the prefrontal cortex,[20] habenula,[18,21] serotonergic raphe,[18] and many other brain regions. However, a mounting body of evidence shows that astrocytes and other glial cells play important roles in the generation of behavior through their modulation of neural circuits.[11] Indeed, studies in humans[22] and animals[23] have raised the possibility that astrocytes might also play important roles in both depression and antidepressant action, but the *in vivo* effects of fast antidepressants on astrocyte physiology have not been described. Recently, astrocyte-like cells[8,24] have been found to drive futility-induced passivity in larval zebrafish,[8] which motivates studying the effects of fast antidepressants in this behavior.

Furthermore, the larval zebrafish's small size and optical transparency have enabled drug discovery[25,26] and brain-wide imaging of neural[27,28] and glial[8] activity at cellular resolution during behavior, approaches that are difficult[20] in conventional rodent assays. Given the similarities between a recently reported futility-induced passivity behavior in larval zebrafish[8] and established rodent FST/TST paradigms, we hypothesized that we could leverage futility-induced passivity in larval zebrafish to develop a scalable behavioral assay, combinable with whole-brain imaging, for the screening of fast-acting antidepressants. **We demonstrate that our assay, which we term the zebrafish futile swimming test (zFST) (1) yields results consistent with other preclinical models of fast antidepressant action and (2) discovers that ketamine-like fast-acting antidepressants drive long-lasting astroglial calcium activity sufficient for their antidepressant effects *in vivo*.**

bioRxiv preprint doi: https://doi.org/10.1101/2022.12.29.522099; this version posted December 29, 2022. The copyright holder for this preprint (which was not certified by peer review) is the author/funder, who has granted bioRxiv a license to display the preprint in perpetuity. It is made available under aCC-BY-NC-ND 4.0 International license.

Ketamine decreases passivity in the zFST

We created the zFST to assay futility-induced passivity in unparalyzed, head-restrained larval zebrafish (Fig. 1a). To that end, we embedded fish in agarose such that their heads were fixed in place and their tails free to move. Using a custom-built behavior rig and software, we detected swimming in real time while delivering visual stimuli consisting of gratings that could move forward or backward. Trials (Fig. 1b) consisted of three different time periods, 'rest,' 'closed loop,' and 'open loop.' During rest periods, gratings were stationary. During closed-loop periods, gratings steadily drifted forward to drive swimming via the optomotor response, a position-stabilizing reflex.[29] If fish swam during closed-loop, the forward-moving gratings would slow down or reverse direction, a visual feedback signaling forward self-motion; thus, a fish's swims are effective during closed-loop. During open-loop, gratings drifted forward with the same velocity as in closed-loop, but swimming did not elicit any visual feedback. In other words, swimming was futile. The open-loop period constitutes an inescapable behavioral challenge as in the rodent FST. Therefore, the key behavioral variable assayed by the zFST is the percentage of the open-loop period spent passive. On the other hand, closed-loop passivity and closed-loop swim rate serve as controls for drugs' potential hyperlocomotion-inducing effects.

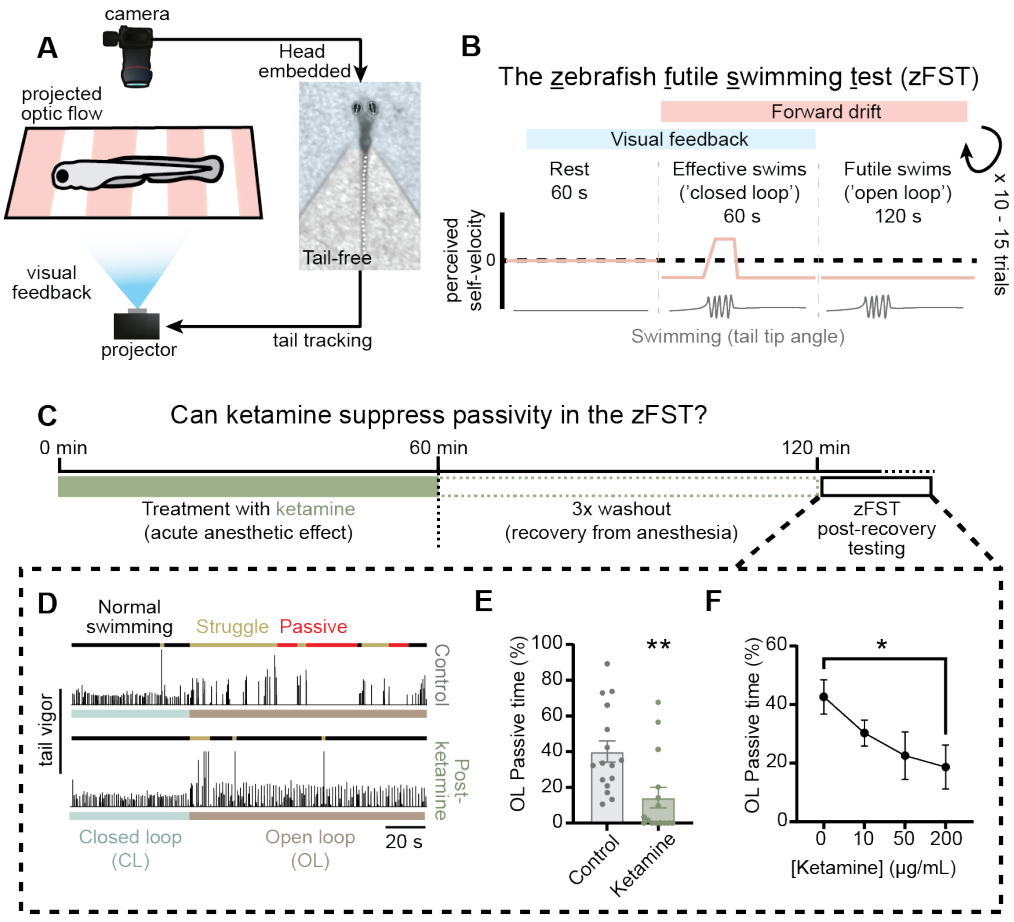

Figure 1. Ketamine suppresses immobility in a futile swimming test for larval zebrafish. (A) Schematic of experimental workflow for imaging swimming behavior in unparalyzed larval zebrafish. Unparalyzed larval zebrafish are imaged and tail posture extracted in real time. Tail posture information is used to control a projector that displays optic flow stimuli (drifting gratings) to drive swimming. (B) Trial structure: 60 s of rest (no stimulus), 60 s of effective swimming ('closed-loop', forward optic flow, visual feedback), then 120 s of futile swimming ('open-loop', forward optic flow, no visual feedback), 10 to 15 repeated trials. (C) Timeline of experiments testing ketamine's effect in the zFST. (D) Example trials for untreated control fish (top) and ketamine-treated fish (bottom). Colors above swim trace indicate normal swimming (black), struggle (yellow), and passivity (red). Colors below swim trace indicate closed- (teal) and open-loop (brown) periods. (E) Ketamine-treated fish spend less time passive (periods ¿ 10 s with no swimming) than untreated controls during open loop. (F) Dose-response curve of ketamine's suppression of open-loop passive time. All error bars denote standard error of the mean (s.e.m.) * $p < 0.05$ ** $p < 0.01$.

As an initial validation, we tested the effects of ketamine on futility-induced passivity in the zFST (Fig. 1c). Ketamine is an NMDA receptor (NMDAR) antagonist widely used

bioRxiv preprint doi: https://doi.org/10.1101/2022.12.29.522099; this version posted December 29, 2022. The copyright holder for this preprint (which was not certified by peer review) is the author/funder, who has granted bioRxiv a license to display the preprint in perpetuity. It is made available under aCC-BY-NC-ND 4.0 International license.

as a rapid-acting dissociative anesthetic. Recent work suggests that at lower doses, after the dissociative effects disappear, ketamine elicits persistent antidepressant action.[1,2] This fast-acting nature and sustained efficacy following a single dose holds great promise as a new approach to MDD.[1] We treated larval zebrafish with ketamine for one hour then allowed them to recover from the acute anesthetic effects for an hour in fish water (Fig. 1c). We then subjected these fish and untreated sibling controls to the zFST. We observed regular swimming in both treated and control fish during closed-loop periods (Fig. 1d, Supplementary Video 1) and in separate experiments in unrestrained fish (Extended Data Fig. 1a-c, Supplementary Discussion). This indicates that ketamine does not cause hyperlocomotion in larval zebrafish. In open-loop, however, we observed that control fish exhibit periods of struggle characterized by larger, uncoordinated tail deflections (Fig. 1d, Extended Data Fig. 1d, Supplementary Video 1) as well as periods of passivity characterized by a lack of swimming (Fig. 1d-e). Therefore, as in the rodent FST/TST, behavioral futility drives passivity in the zFST. Notably, ketamine treatment significantly decreased passivity during open-loop (Fig. 1d-e, Supplementary Video 2) in a dose-dependent manner (Fig. 1f). This decrease in passivity was not due to an inability of fish to struggle or distinguish closed from open loop (Extended Data Fig. 1e), nor was it due to motor rebound from anesthesia (Extended Data Fig. 2, Supplementary Discussion). These results are consistent with observations made in a previously published passive coping behavior in older zebrafish[18] as well as in the rodent FST/TST.

zFST generalizability and specificity

To characterize the generalizability and specificity of the zFST, we tested the effects of a variety of fast-acting and classical antidepressants (Fig. 2a, Extended Data Fig. 3). We found that previously reported fast antidepressants targeting either NMDA receptor (ketamine, MK-801, DXM) (Fig. 2b, Extended Data Fig. 3a) or serotonergic (DOI) (Fig. 2c) signaling decreased passivity in the zFST. We also tested a 5-HT2A receptor agonist, TCB-2,[30] that to our knowledge has not been characterized in rodent passivity models. TCB-2 treatment likewise resulted in a suppression of passivity in the zFST (Fig. 2c), so we predict that it, similarly to other psychedelics like LSD, DOI and psilocybin,[31,32] could have antidepressant effects in other models. One of the drawbacks for therapeutic use of ketamine and classical psychedelics is their potential for hallucinogenic effects. This has led to the generation of psychedelic analogs with diverse chemical structures and pharmacological targets that are predicted to reduce these dissociative effects.[33–35] We found that these compounds also significantly reduce passivity in the zFST (Fig. 2a, Extended Data Fig. 3b-c)), validating our assay for this new generation of antidepressant compounds and demonstrating a conservation of their effects across species.

By contrast, consistent with their lack of single-dose antidepressant effects in rodents and humans, the classical antidepressants fluoxetine or (S)-citalopram (SSRIs) and desipramine (TCAs) showed no passivity-suppressing effects after a single, one-hour dose (Fig. 2d). Interestingly, (2R,6R)-hydroxynorketamine, a pharmacologically inert[36] metabolite of ketamine that has been reported to decrease passivity in the rodent FST,[9] had no effect on passivity in the zFST (Extended Data Fig. 3d), raising the possibility that it acts through pathways not found in the larval zebrafish and separate from ketamine's action. Finally, as an additional test of specificity, we assayed NMDAR antagonists that have no reported antidepressant effects in humans. These compounds are memantine, a low-affinity antagonist binding the same site as ketamine/MK-801, and AP5, a competitive antagonist with a different binding site. Although AP5-like compounds have been reported to have antidepressant effects in rodent FST models,[37] we found that AP5 did not significantly decrease passivity in the zFST (Extended Data

bioRxiv preprint doi: https://doi.org/10.1101/2022.12.29.522099; this version posted December 29, 2022. The copyright holder for this preprint (which was not certified by peer review) is the author/funder, who has granted bioRxiv a license to display the preprint in perpetuity. It is made available under aCC-BY-NC-ND 4.0 International license.

Fig. 3e). Similarly, replicating results in rodents,[38] we found a similar lack of effect for memantine (Extended Data Fig. 3f). Thus, our assay can distinguish between different compounds that all target the same receptor but bind different sites.

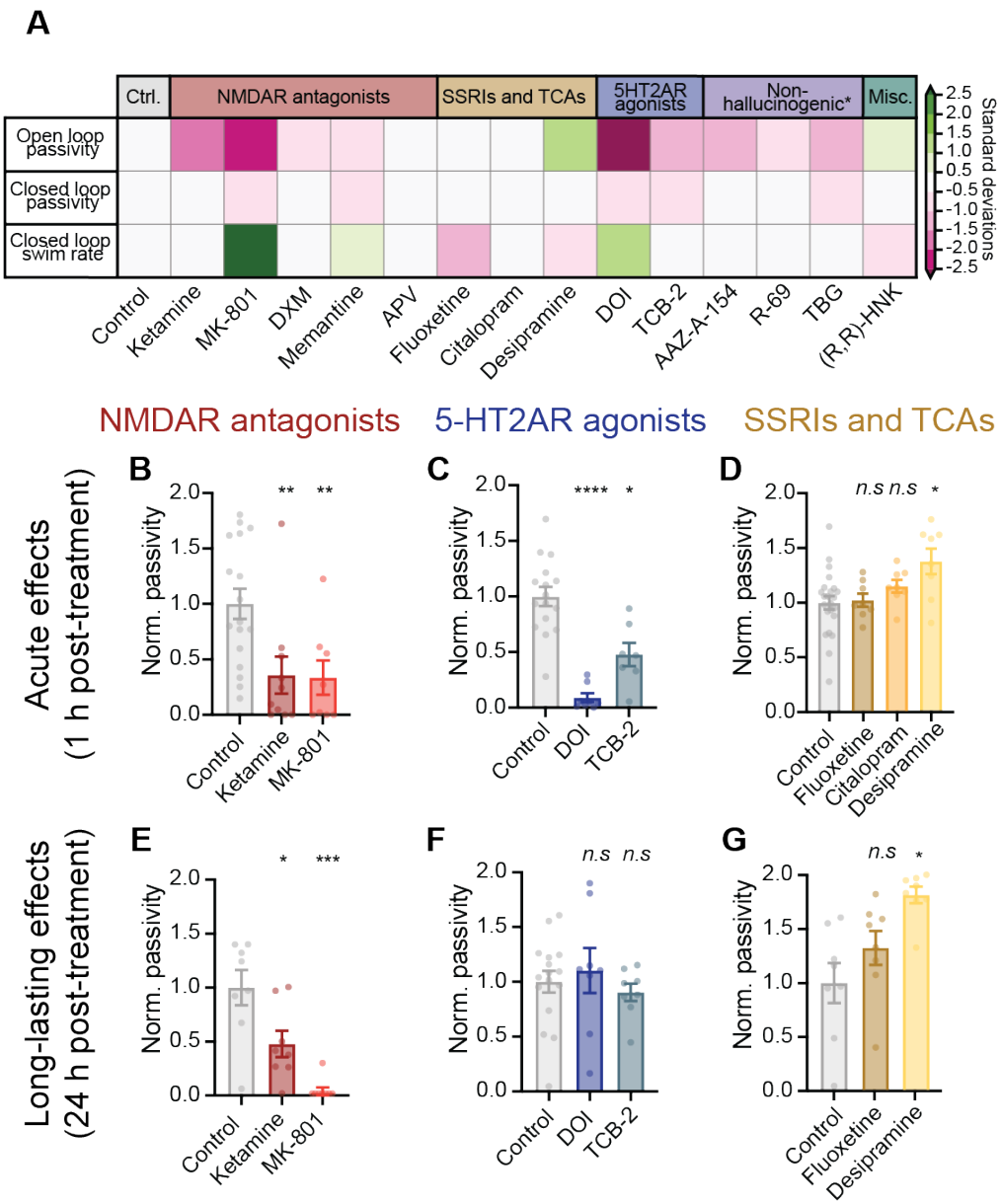

Figure 2. The zFST enables selective screening of fast-acting antidepressant compounds with diverse pharmacological targets. (A) Open-loop passivity, closed-loop passivity, and closed-loop swim rate of fish treated with vehicle (control) or various different pharmacological compounds (normalized to mean of control) in the zFST. Results are grouped by major pharmacological target of treatment compound. (B-D) Acute (1 h post-washout) effects of (B) Phencyclidine-site NMDA receptor antagonists, (C) 5-HT2A receptor agonists, and (D) selective serotonin reuptake inhibitors (SSRIs) and tricyclic antidepressants (TCAs) on open-loop passivity. Phencyclidine-site NMDA receptor antagonists and 5-HT2A receptor agonists exhibit acute passivity-suppressing effects, but SSRIs and TCAs do not. (E-G) Persistent (24 h post-washout) effects of (B) Phencyclidine-site NMDA receptor antagonists, (C) 5-HT2A receptor agonists, and (D) SSRIs and TCAs on open-loop passivity. Only the phencyclidine-site NMDA receptor antagonists exhibit persistent passivity suppressing effects in the zFST. All error bars denote s.e.m. n.s. $p > 0.05$, * $p < 0.05$, ** $p < 0.01$, *** $p < 0.005$, **** $p < 0.001$.

In addition to fast-acting effects, we also assayed compounds' persistent effects on passivity by testing animals in the zFST twenty-four hours after treatment (Fig. 2e-g). We found that in our assay, of the drugs tested only the phencyclidine-site NMDAR antagonists ketamine and MK-801 retained a passivity-suppressing effect after 24 h (Fig. 2e). In contrast, the classical antidepressants we tested showed no long-lasting effect following a single dose (Fig. 2g). Surprisingly, however, while the psychedelic 5-HT2AR agonists we tested exhibited a strong acute suppression in passivity, we observed no passivity suppressing effect in the zFST after 24 h (Fig. 2f). These results suggest that,

bioRxiv preprint doi: https://doi.org/10.1101/2022.12.29.522099; this version posted December 29, 2022. The copyright holder for this preprint (which was not certified by peer review) is the author/funder, who has granted bioRxiv a license to display the preprint in perpetuity. It is made available under aCC-BY-NC-ND 4.0 International license.

although phencyclidine-site NMDAR antagonists and psychedelics drive some convergent changes in neural physiology, including enhanced plasticity and spinogenesis,[39,40] they might act through different circuits or pathways to drive long-term suppression of depressive symptoms.

Ketamine elevates Ca^{2+} in astroglia

The larval zebrafish, due to its optical accessibility, offers unique opportunities for observing how fast antidepressants affect the dynamics of neurons and non-neuronal cells across the entire brain. To illustrate the power of this approach, we performed brain-wide imaging during the administration of compounds that possessed acute passivity-suppressing effects (Fig. 3). Because radial astrocytes have been shown to drive futility-induced passivity in zebrafish,[8] we focused on calcium activity in radial astrocytes during and after ketamine treatment (Fig. 3a, Extended Data Fig. 4a).

Strikingly, acute exposure to ketamine induced a prolonged rise in astroglial cytosolic calcium concentration (Fig. 3b-d, Supplementary Video 3), with elevated calcium levels lasting over 20 minutes (Extended Data Fig. 4b). Consistent with its pharmacological profile similar to ketamine, the phencyclidine-site NMDAR antagonist MK-801 also increased cytosolic calcium in astroglia to a similar extent as ketamine (Fig. 3e). In contrast to the effects of ketamine and MK-801, the classical antidepressant fluoxetine, the psychedelic DOI, and the anesthetic MS-222 did not elevate cytosolic calcium in astroglia (Fig. 3e). These functional data further support our hypothesis that fast antidepressants targeting NMDA receptors might act through different pathways from those targeting 5-HT2A receptors and invite speculation that physiological changes in astroglia resulting from the long-lasting calcium signaling triggered by phencyclidine-site NMDAR antagonists might contribute to their sustained passivity-suppressing effects.

Ketamine and MK-801 both elevated astroglial calcium, but they had different effects on neural activity (Extended Data Fig. 5). While

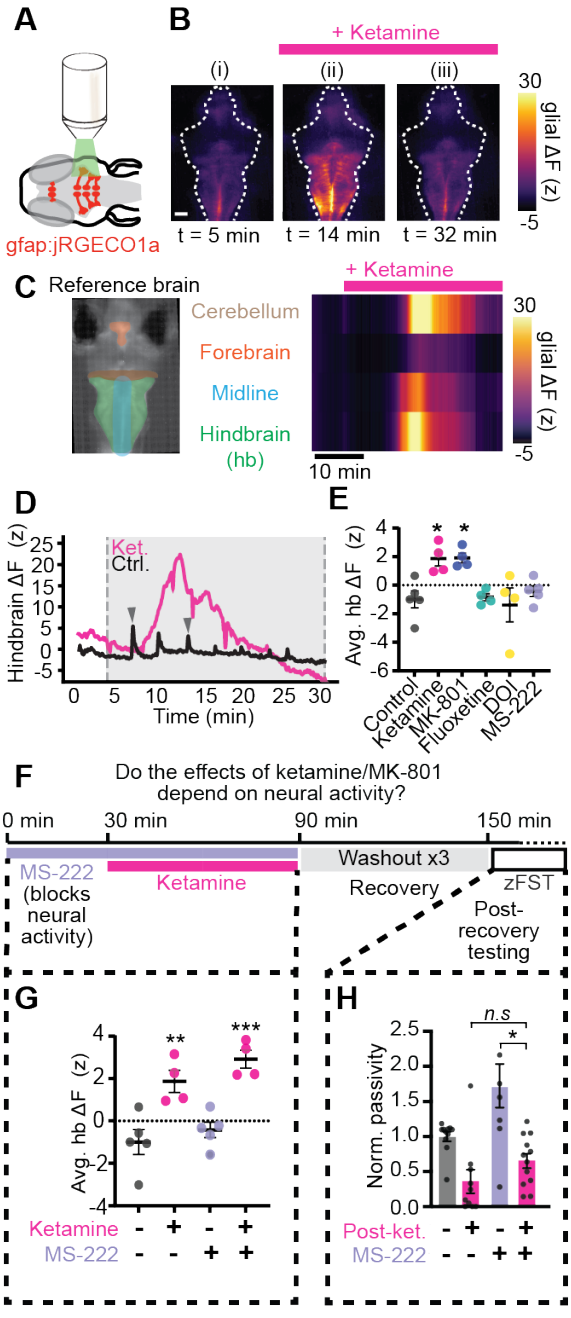

Figure 3. Ketamine triggers a long-lasting calcium elevation in astroglia independent of neural activity. (A) Fish expressing the calcium indicator jRGECO1a in astroglia were imaged using an epifluorescence microscope. (B) Fluorescence micrographs of jRGECO1a signal in an example fish at three time points illustrating elevation and return to baseline of cytosolic calcium in presence of ketamine. Scale bar 50μm. (C) Heatmap of glial jRGECO1a signal in four ROIs (left) for fish in (B). Pink bar indicates ketamine in bath. (D) Hindbrain jRGECO1a fluorescence change in an example fish treated with ketamine or vehicle (control). Short increases in astrocytic calcium during struggles in control fish are indicated by gray arrowheads. (E) Average hindbrain fluorescence change following treatment with listed compounds. Ketamine or MK-801 (NMDAR antagonists), but not fluoxetine (SSRI), DOI (5-HT2AR agonist), or MS-222 (anesthetic), elevate cytosolic astroglial calcium. (F) Timeline of experiments testing whether neural activity is required for the effects of ketamine. (G) Hindbrain jRGECO1a fluorescence change following treatment with ketamine alone, MS-222 alone, or ketamine and MS-222 together; both elevate astroglial cytosolic calcium. *(cont. next page)*

bioRxiv preprint doi: https://doi.org/10.1101/2022.12.29.522099; this version posted December 29, 2022. The copyright holder for this preprint (which was not certified by peer review) is the author/funder, who has granted bioRxiv a license to display the preprint in perpetuity. It is made available under aCC-BY-NC-ND 4.0 International license.

Figure 3 (cont.) (H) Open-loop passivity in zFST for fish treated with ketamine, with or without neural activity blocker MS-222. Ketamine still suppresses passivity in the presence of MS-222. Data for ketamine alone is the same as in Fig 2B and is repeated here for comparison. First three conditions are repeated from Fig. 3E for comparison. All error bars denote s.e.m. n.s. $p > 0.05$, $^{*}p < 0.05$, $^{**}p < 0.01$, $^{***}p < 0.001$. F (z) for each fish was calculated as the difference between mean total fluorescence before treatment subtracted to total fluorescence at a specific time point, divided by the standard deviation of total fluorescence before treatment, for each mask, C, or hindbrain mask E,G.

ketamine quickly inhibited neural activity across the brain (Extended Data Fig. 5a-c), MK-801 lacked such an inhibitory effect (Extended Data Fig. 5d-e). How can two compounds with such different acute effects on neural activity both lead to the same passivity-suppressing effect in the zFST? The similar stimulatory effects of MK-801 and ketamine on astroglial calcium, despite different effects on neural activity, led us to hypothesize that phencyclidine-site NMDAR antagonists could act through astroglia in a neural activity-independent manner.

To investigate the relative contributions of astroglial versus neural activity in mediating the effects of these compounds, we tested the behavioral effects of ketamine and MK-801 in fish anesthetized with the sodium channel blocker MS-222 (Fig. 3f-h). Treatment with MS-222 quickly suppressed neuronal activity in most brain areas (Extended Data Fig. 6a-b) and occluded the acute effects of ketamine or MK-801 on neuronal activity. However, ketamine and MK-801 still suppressed passivity in the zFST when administered during anesthesia (Fig. 3h, Extended Data Fig. 6c). This result suggests that changes in spiking activity in neurons during the treatment of ketamine or MK-801 is not necessary for the compounds' passivity-suppressing effects. Remarkably, ketamine treatment under anesthesia still caused glial calcium elevation in the hindbrain similar to the calcium elevation observed in the absence of anesthesia (Fig. 3g). We interpret this unexpected result as indicating that ketamine's effects on glial calcium are largely or fully independent of neural activity. The neural activity-independent effects of ketamine's action may explain clinical observations that ketamine has antidepressant effects even when administered under general anesthesia.[41]

Glial Ca^{2+} sufficient to lower passivity

Finally, we tested whether elevations in astroglial calcium, similar to the rise we observed during ketamine treatment, were sufficient to suppress passivity in the zFST after recovery. During futility-induced passivity, futile swims trigger norepinephrine release, and norepinephrine drives an accumulation of calcium in hindbrain astroglia.[8] Therefore, we optogenetically activated norepinephrinergic neurons to elevate calcium in astroglia (Fig. 4, Extended Data Fig. 7). As previously reported,[8] activation of NE neurons expressing CoChR (Extended Data Fig. 7a-b) with blue (488 nm) light induced a calcium rise in hindbrain radial astroglia similar to the increase in calcium observed with ketamine but with a shorter duration Extended Data Fig. 7c-d). We found that continuous stimulation of norepinephrinergic (NE) neurons for half an hour (Fig. 4a) led to decreased passivity in the zFST (Fig. 4b) after an hour of recovery. Because norepinephrine acts on neurons in addition to glia, we also chemogenetically activated astroglia directly by generating a fish line expressing the rat transient receptor potential V1 channel (TRPV1) in glia (Extended Data Fig. 7e). Native TRPV1 in zebrafish is not sensitive to the chemical capsaicin. On the other hand, rat TRPV1 is activated by capsaicin, leading to an influx of calcium; this approach has previously been validated in radial astrocytes.[8,42] We found that capsaicin treatment of fish expressing TRPV1 in astroglia for 30 minutes (Fig. 4c) also suppressed passivity in the zFST an hour after washout (Fig. 4d-e). Altogether, these data suggest that the aftereffects of long-lasting calcium elevation in astroglia, similar to those observed following treatment with ketamine, are sufficient to suppress passivity in an assay for behavioral despair.

While acute increases in glial calcium during futile swimming drive passivity, the aftereffects of much larger and longer elevations evoked by the application of ketamine, and by our other manipulations, suppress passivity following recovery. To reconcile the seemingly contradictory effects of astroglial calcium during futile swimming and during ketamine administration, we hypothesized that although ketamine drives cytosolic calcium elevation when administered, when astroglial calcium later returns to baseline following washout and recovery, astroglia are less responsive to futile swims. If this

bioRxiv preprint doi: https://doi.org/10.1101/2022.12.29.522099; this version posted December 29, 2022. The copyright holder for this preprint (which was not certified by peer review) is the author/funder, who has granted bioRxiv a license to display the preprint in perpetuity. It is made available under aCC-BY-NC-ND 4.0 International license.

is the case, then futile swimming should evoke smaller calcium transients in astroglia after recovery from ketamine treatment than before ketamine treatment. To test our hypothesis, we imaged futile swimming-induced transients prior to, and after ketamine treatment (Fig. 4f), in addition to the effects of the treatment itself. Consistent with previous report,[8] we observed that futile swims evoked astroglial calcium transients (Fig. 4g). Ketamine treatment resulted in a large sustained calcium elevation (Fig. 4h) as shown in Figure 3. By contrast, following washout and recovery, futile swimming elicited much smaller calcium transients (Fig. 4i-j). These data support our hypothesis that ketamine exerts its passivity-suppressing aftereffects through suppression of astroglial calcium signaling pathways sensitive to behavioral futility. The precise mechanism of this suppression remains to be discovered. Interestingly, astrocytic calcium is also recruited by transcranial direct current stimulation (tDCS) in rodents,[43] and the antidepressant effects of tDCS require many of the same molecular components as the glial futility pathway in larval zebrafish,[8] suggesting that ketamine might act through similar pathways.

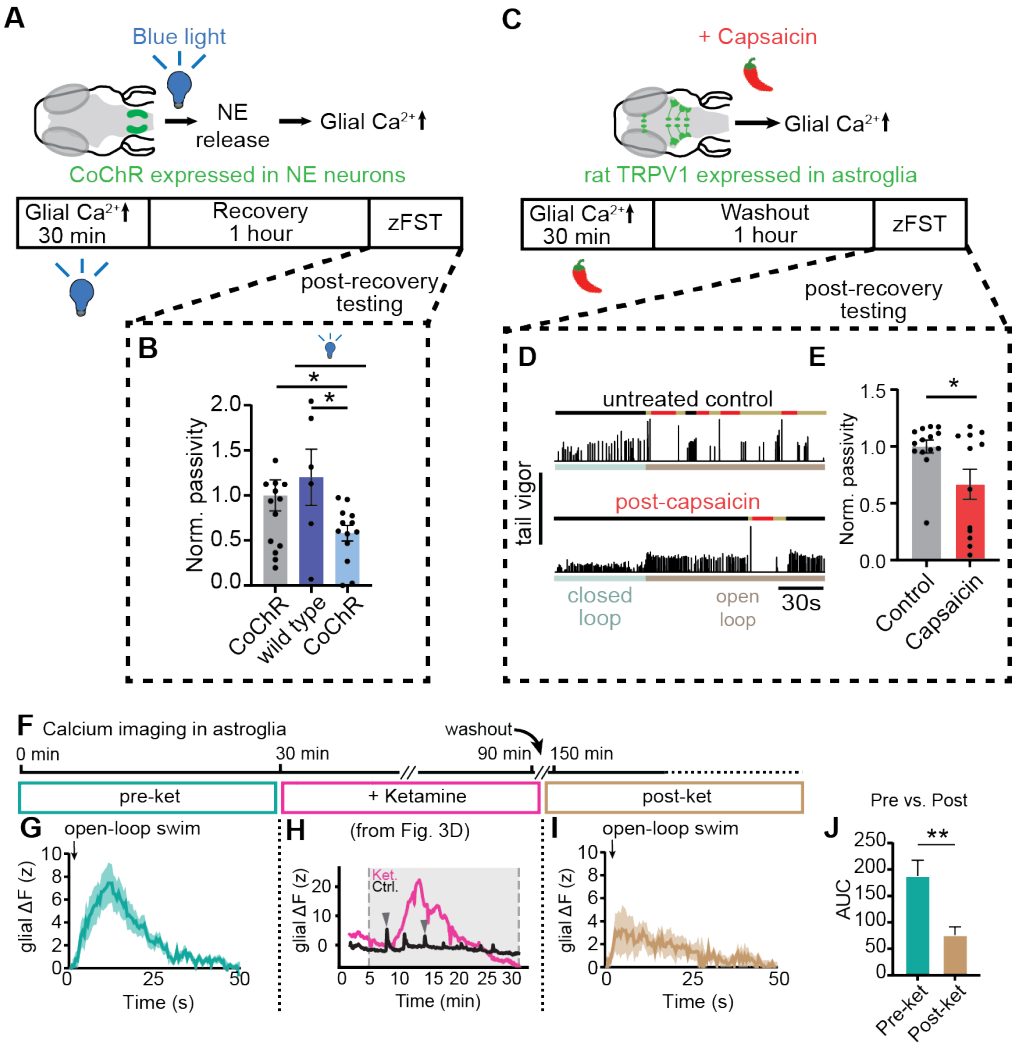

Figure 4. Elevations in astroglial calcium are sufficient to suppress futility-induced passivity after recovery. (A) Timeline for experiments testing effects of stimulating glial calcium by activating norepinephrinergic (NE) neurons. Transgenic fish expressing the channelrhodopsin CoChR in norepinephrinergic (NE) neurons were continually stimulated optogenetically with blue (488 nm) light for 30 minutes. Fish were allowed to recover for an hour then assayed for futile swimming in the zFST. (B) Passivity normalized to sibling, non-stimulated controls. Optogenetic stimulation suppressed passivity in the zFST following recovery compared to non-stimulated sibling controls and non-expression controls stimulated with blue light. (C) Timeline for experiments testing effects of stimulating glial calcium directly through chemogenetics, Transgenic fish expressing rat TRPV1 in astroglia were treated with capsaicin for 30 min. After 30 min, capsaicin was washed out and fish allowed to recover for 1 h before being tested in the zFST. (D) Example swimming of capsaicin-treated fish (bottom) and untreated sibling controls (top). Black, yellow, and red segments above swim vigor trace denote regular swimming, struggling, and passivity, respectively. *(cont. next page)*

bioRxiv preprint doi: https://doi.org/10.1101/2022.12.29.522099; this version posted December 29, 2022. The copyright holder for this preprint (which was not certified by peer review) is the author/funder, who has granted bioRxiv a license to display the preprint in perpetuity. It is made available under aCC-BY-NC-ND 4.0 International license.

Figure 4 (Cont.) (E) Passivity normalized to untreated sibling controls. Capsaicin-treated fish exhibit decreased passivity in the zFST, although the distribution of passivity duration is bimodal. (F) Timeline of imaging experiments to compare acute futility-induced calcium signaling in astroglia before and after ketamine treatment. Three periods correspond to imaging periods for panels G-I. (G) Open-loop swim-triggered jRGECO1a signal in hindbrain glia before ketamine treatment. (H) Same graph shown in Fig. 3D reproduced here for comparison with panels G and I. Note horizontal scale in minutes rather than seconds. (I) Open-loop swim-triggered jRGECO1a signal in hindbrain glia after ketamine treatment. (J) Area under the curve (AUC) for jRGECO1a signal following struggles in fish before and after treatment. All error bars denote s.e.m. $^{*}p < 0.05$, $^{**}p < 0.01$

Discussion

Rapid-acting antidepressants exert their effects by modulating the activity of many brain regions, including the habenula,[18,21] serotonergic system,[18] and prefrontal cortex.[20] These drugs also bind a diverse array of molecular targets[10,44,45] to elicit changes in structural plasticity[10,39,40] and physiology.[21] However, a framework that connects the molecular and cellular effects of fast-acting antidepressants to their effects on circuit dynamics remains lacking. Our work provides evidence that ketamine drives ultra-long cytosolic calcium elevation in a population of hindbrain astroglial cells that integrate futility and drive a behavioral state transition from active struggle to passivity.[8] This calcium elevation drives changes in astroglial physiology that persist even when calcium has returned to baseline and ketamine is no longer in the brain; astroglial responsiveness to futility is blunted. Because the activation of astroglia in response to futility leads to widespread inhibition of neural activity that accounts motor suppression,[8] our work provides one mechanism through which the cell-physiological effects of ketamine can explain its effects on circuit function and behavior.

The development of the forced swimming and tail suspension tests in rodents over four decades ago marked an important step in the preclinical study of antidepressant action. The FST and TST have been widely used since their inception to identify putatively antidepressant compounds and to study the mechanisms through which those compounds act. Indeed, behavioral pharmacology done using the FST has played an important role in the study of how fast-acting antidepressants like ketamine function.[2,9,10,40] We believe that our development of an analog of the FST for larval zebrafish constitutes a similar advance for the larval zebrafish as a model system, with two much broader implications for behavioral pharmacology and the neurobiology of depression and antidepressant action:

(1) Our results connect the fields of glial biology and the neurobiology of depression. Using our assay, we observed an unexpected stimulatory effect of the fast antidepressant ketamine on astroglial calcium *in vivo*. Important work has previously described changes to astrocyte physiology in depression,[23] but ketamine is thought to act primarily on neurons to exert its antidepressant action.[21] Our results challenge this prevailing view by showing that ketamine and ketamine-like drugs directly affect astroglial physiology, likely counteracting the dysfunction that arises in depression. While we presented evidence that the aftereffects of elevating cytosolic calcium in astroglia are sufficient to suppress passivity, how ketamine drives calcium signaling in astroglia, what changes occur to neural and glial physiology as a consequence, and whether these mechanisms are conserved in other species, remain important open questions. Understanding how fast-acting antidepressants act on non-neuronal cell types, in addition to neurons, will lead to insight on the cellular and circuit pathways that go awry during major depressive disorder and will inform the discovery and rational design of new fast and effective therapeutics.

(2) Larval zebrafish have long been used for drug discovery and behavioral profiling in high-throughput assays for simple behavioral phenotypes.[25] Here we show that larval zebrafish can also be used to assay complex behavioral phenotypes, including those implicated in psychiatric disorders like depression, in ways that are higher-throughput than in rodent counterparts. Furthermore, the optical and genetic accessibility of the larval zebrafish presents a unique opportunity to investigate the effects of antidepressants on both neurons and non-neuronal cells in the brain,[46] not only *in vivo* but in the behaving animal. Because larval zebrafish survive and behave for many hours following head-fixation, the effects of these compounds can be studied over many timescales. In addition, because the entire body of the fish is transparent, it could serve as a model for the effects of antidepressants on the peripheral nervous system and other organ systems in the future to identify the physiological mechanisms by which the many side effects of

bioRxiv preprint doi: https://doi.org/10.1101/2022.12.29.522099; this version posted December 29, 2022. The copyright holder for this preprint (which was not certified by peer review) is the author/funder, who has granted bioRxiv a license to display the preprint in perpetuity. It is made available under aCC-BY-NC-ND 4.0 International license.

classical and fast antidepressants manifest.[47,48] The conserved effects of antidepressants from fish to mammals, together with the genetic and optical accessibility of the larval zebrafish, hold promise for understanding the underlying mechanisms from the molecular to the body-wide scale.

bioRxiv preprint doi: https://doi.org/10.1101/2022.12.29.522099; this version posted December 29, 2022. The copyright holder for this preprint (which was not certified by peer review) is the author/funder, who has granted bioRxiv a license to display the preprint in perpetuity. It is made available under aCC-BY-NC-ND 4.0 International license.

Acknowledgments

We would like to thank Dr. Bryan Roth and Dr. Jon Ellman, and their labs, for providing us with R-69. We would like to thank Herriet Hsieh for discussions and comments on the manuscript. We would also like to thank Sabrina Boutselis for designing the red hot chili pepper illustration. The *bioRxiv* version of this manuscript was formatted using a template by Philipp Schlegel.

Funding:

Howard Hughes Medical Institute (ABC, SN, MBA)
NIH Grant U19NS104653 (FE)
NIH Grant 1R01NS124017 (FE)
NIH Grant 1R01GM128997 (DEO)
NSF Grant IIS-1912293 (FE)
NSF GRFP DGE1745303 (ABC)
Simons Foundation SCGB 542943SPI (FE, MBA)

Author contributions:

Conceptualization: MD, ABC, MCF, MBA
Methodology: MD, ABC, SN
Investigation: MD, ABC
Visualization: MD, ABC
Funding acquisition: DEO, MCF, FE, MBA
Project administration: FE, MBA
Supervision: DEO, MCF, FE, MBA
Writing – original draft: MD, ABC
Writing – edit and revision: MD, ABC, DEO, MCF, FE, MBA

Methods

Experimental model and subject details. Experiments were conducted according to the guidelines of the National Institutes of Health and were approved by the Standing Committee on the Use of Animals in Research of Harvard University. Animals were handled according IACUC protocols 2729 (Engert lab), 18-11-340-1 (Fishman lab), and 22-0216 (Ahrens lab). For all experiments, we used wild-type larval zebrafish (strains AB, WIK or TL), aged 5–8days post-fertilization (dpf). We did not determine the sex of the fish we used since it is indeterminate at this age. Fish were raised in shallow Petri dishes and fed ad libitum with paramecia after 4 dpf. Fish were raised on a 14 h:10 h light:dark cycle at around 27°C. All experiments were done during daylight hours (4–14h after lights on). All protocols and procedures were approved by the Harvard University/Faculty of Arts and Sciences Standing Committee on the Use of Animals in Research and Teaching (Institutional Animal Care and Use Committee) and the Janelia Institutional Animal Care and Use Committee.

Fish lines.
For all behavioral experiments we used:
Wild type - strains AB and WIK: all panels of Fig. 1, all panels of Fig. 2, Fig. 3F-H, Fig. S1-3.
For imaging of astroglial calcium we used:
Cytosolic, red calcium indicator. *Tg(gfap:jRGECO1a):* Fig. 3A-E, Fig. S4F-G[8,49]
For imaging of neuronal calcium we used:
Nuclear-localized, green calcium indicator. *Tg(elavl3:H2B-jGCaMP7f)^{jf90}:* Fig. S4A-E[50]
For optogenetic activation of norepinephrinergic neurons we used:
Channelrhodopsin expressed under dbh promoter. *Tg(dbh:KalTA4);Tg(UAS:CoChR-eGFP):* Fig. 4A-B, Fig. S5A-D[51]
For chemogenetic activation of astroglia we used:

bioRxiv preprint doi: https://doi.org/10.1101/2022.12.29.522099; this version posted December 29, 2022. The copyright holder for this preprint (which was not certified by peer review) is the author/funder, who has granted bioRxiv a license to display the preprint in perpetuity. It is made available under aCC-BY-NC-ND 4.0 International license.

Rat transient receptor potential cation channel subfamily V member 1 (TRPV1) expressed under gfap promoter. *Tg(gfap:TRPV1-T2A-eGFP)^{jf64}:* Fig. 4C-E, Fig. S5E (this paper)

Transgenesis. We generated the *Tg(gfap:TRPV1-T2A-eGFP)^{jf64}* line for use in our chemogenetic activation experiments. The line was generated in casper background[52] using the Tol2 method.[53]

Embedding of larval zebrafish for tail-tracking experiments. Larval zebrafish aged 6-8 dpf were embedded in small round Petri dishes (e.g. Corning 351006); importantly, dishes should not be tissue culture-treated to allow agarose to adhere. Solutions of 2% low melting-point agarose (Sigma-Aldrich A9414) were prepared by heating powdered agarose in system water and agitating until solution was clear. The 2% agarose solution was kept at 42-48 degrees Celsius. To embed fish, a small amount of 2% agarose solution was pipetted in the middle of a Petri dish. A larval zebrafish was then transferred, using either a small glass or Pasteur pipette, taking care to minimize addition of water to the agarose solution during transfer. Using either small forceps or a small ($\sim 10 - 100\,\mu L$) plastic micropipette tip, larval zebrafish were gently rotated until they were dorsal side up. Fish often struggle when transferred to the agarose solution, so care should be taken to keep fish righted until agarose solidifies. Once the agarose solidified, we freed the tail of the fish by carefully cutting away the hardened agarose around the tail with a micro-scalpel (Fine Science Tools 10315-12). Care should be taken to remove enough agarose to prevent the tail from hitting or becoming stuck on agarose during swimming or struggle.

Pharmacological treatment of larval zebrafish. Approximately 10-20 larval zebrafish aged 6-8 dpf were transferred to single wells in 12-well plates containing 2 mL of fish water (8-12 fish/well). Quantities of either the experimental pharmacological compound (Table S1) or vehicle control were added and fish were incubated for one hour. Fish were then washed three times in a larger Petri dish and then allowed to recover for one hour, following which experimentation would begin.

Tail-tracking of embedded larval zebrafish and visual stimulus. For all behavioral experiments involving embedded larval zebrafish, we used a previously published, custom-build behavioral rig and custom-written code.[54] Briefly, we illuminated the fish and its environment using infrared light-emitting diode panels (wavelength $940nm$, Cop Security). The tail-posture of the fish was tracked using a camera (Grasshopper3-NIR, FLIR Systems) with a zoom lens (Zoom 7000, 18–108 mm, Navitar) and a long-pass filter (R72, Hoya). We determined the posture of the tail, as well as its tip angle, by analyzing the position of ~ 25 equally spaced, user-defined key points along its length. Posture was determined and recorded in real-time at 90 Hz using custom-written Python scripts (Python 3.7, OpenCV 4.1).

Tracking of freely swimming larval zebrafish. For all behavioral experiments involving freely-swimming larval zebrafish, we also used a previously published, custom-build behavioral rig and custom-written code.[54] The illumination and detection of freely swimming fish used the same behavioral rigs as described for embedded fish. To track the position of fish and determine swim bouts in real time at 90 Hz, we used custom-written Python scripts (Python 3.7, OpenCV 4.1). The background of the camera image was subtracted and the body of the fish identified by center of mass. Orientation was determined as the axis of largest pixel variance in the identified body. Swim bouts were detected by computing a 50 ms rolling variance and identifying thresholded peaks.

Passivity computation. Passive periods were operationally defined to be periods greater than 10 s in length in which the fish did not perform a swim bout. To determine the percentage of the open-loop interval spent passive per trial, the total length of all passive periods within the open-loop interval of a trial was summed and the sum divided by the length of the open-loop interval. The same computation was performed to determine passive fraction for closed-loop intervals as well.

Epifluorescence imaging of neurons and radial astrocytes. Larval zebrafish aged 6-8 dpf were embedded in small round petri dishes and their tails freed as described previously. To image neurons, we used previously published fish lines *Tg(elavl3:H2B-GCaMP7f)* for neural imaging and *Tg(gfap:jRGECO1a)* for astroglial imaging. Imaging was performed using a dissecting microscope (Olympus MVX10) with a CMOS camera (IDS Imaging UI-3370CP-NIR) and an LED

bioRxiv preprint doi: https://doi.org/10.1101/2022.12.29.522099; this version posted December 29, 2022. The copyright holder for this preprint (which was not certified by peer review) is the author/funder, who has granted bioRxiv a license to display the preprint in perpetuity. It is made available under aCC-BY-NC-ND 4.0 International license.

lamp for fluorescent imaging (X-Cite 120 LED mini). For analysis, each video frame was registered to a reference brain using OpenCV and fluorescence in each defined brain region was extracted with manually segmented masks. Fluorescence Z-score was calculated as the difference between mean total fluorescence before treatment subtracted to average baseline fluorescence, divided by the standard deviation of total fluorescence before treatment, for each mask.

Optogenetic and chemogenetic activation experiments. For the optogenetic experiments, *Tg(dbh:CoChR-eGFP)*[51,55] fish were incrossed and their larvae raised until 6-8 dpf. Fish were screened using an epifluorescence scope and selected according to the GFP signal in NE-MO cells, and raised to 6-8 dpf. Positive fish were then placed on top of a 16x16 blue LED matrix and stimulated for 30 minutes with blue light (0.3W, Newegg 9SIA9DCJ4V0029) or control ambient light. After 1h recovery, fish were assayed in the zFST. For the chemogenetic experiments, *Tg(gfap:TRPV1-T2A-eGFP)*^{jf64} were crossed with WT fish from a casper background. Fish were screened using an epifluorescence scope and selected according to the GFP signal in hindbrain and spinal cord glia, and raised to 6-8 dpf. Positive fish were then incubated with 2 μM capsaicin (Sigma 12084) in fish water (0.025% DMSO final concentration) or an equivalent concentration of vehicle for 20-30 minutes. Fish were then washed and placed in fresh fish water. After 1h recovery, fish were assayed in the zFST.

References

1. R M Berman, A Cappiello, A Anand, D A Oren, G R Heninger, D S Charney, and J H Krystal. Antidepressant effects of ketamine in depressed patients. *Biol. Psychiatry*, 47(4):351–354, February 2000.
2. Anita E Autry, Megumi Adachi, Elena Nosyreva, Elisa S Na, Maarten F Los, Peng-Fei Cheng, Ege T Kavalali, and Lisa M Monteggia. NMDA receptor blockade at rest triggers rapid behavioural antidepressant responses. *Nature*, 475(7354):91–95, June 2011.
3. Alan K Davis, Frederick S Barrett, Darrick G May, Mary P Cosimano, Nathan D Sepeda, Matthew W Johnson, Patrick H Finan, and Roland R Griffiths. Effects of Psilocybin-Assisted therapy on major depressive disorder: A randomized clinical trial. *JAMA Psychiatry*, 78(5):481–489, May 2021.
4. M E Seligman and S F Maier. Failure to escape traumatic shock. *J. Exp. Psychol.*, 74(1):1–9, May 1967.
5. Steven F Maier and Martin E P Seligman. Learned helplessness at fifty: Insights from neuroscience. *Psychol. Rev.*, 123(4):349–367, July 2016.
6. R D Porsolt, A Bertin, and M Jalfre. Behavioral despair in mice: a primary screening test for antidepressants. *Arch. Int. Pharmacodyn. Ther.*, 229(2):327–336, October 1977.
7. L Steru, R Chermat, B Thierry, and P Simon. The tail suspension test: a new method for screening antidepressants in mice. *Psychopharmacology*, 85(3):367–370, 1985.
8. Yu Mu, Davis V Bennett, Mikail Rubinov, Sujatha Narayan, Chao-Tsung Yang, Masashi Tanimoto, Brett D Mensh, Loren L Looger, and Misha B Ahrens. Glia accumulate evidence that actions are futile and suppress unsuccessful behavior. *Cell*, 178(1):27–43.e19, June 2019.
9. Panos Zanos, Ruin Moaddel, Patrick J Morris, Polymnia Georgiou, Jonathan Fischell, Greg I Elmer, Manickavasagom Alkondon, Peixiong Yuan, Heather J Pribut, Nagendra S Singh, Katina S S Dossou, Yuhong Fang, Xi-Ping Huang, Cheryl L Mayo, Irving W Wainer, Edson X Albuquerque, Scott M Thompson, Craig J Thomas, Carlos A Zarate, Jr, and Todd D Gould. NMDAR inhibition-independent antidepressant actions of ketamine metabolites. *Nature*, 533(7604):481–486, May 2016.
10. Plinio C Casarotto, Mykhailo Girych, Senem M Fred, Vera Kovaleva, Rafael Moliner, Giray Enkavi, Caroline Biojone, Cecilia Cannarozzo, Madhusmita Pryiadrashini Sahu, Katja Kaurinkoski, Cecilia A Brunello, Anna Steinzeig, Frederike Winkel, Sudarshan Patil, Stefan Vestring, Tsvetan Serchov, Cassiano R A F Diniz, Liina Laukkanen, Iseline Cardon, Hanna Antila, Tomasz Rog, Timo Petteri Piepponen, Clive R Bramham, Claus Normann, Sari E Lauri, Mart Saarma, Ilpo Vattulainen, and Eero Castrén. Antidepressant drugs act by directly binding to TRKB neurotrophin receptors. *Cell*, 184(5):1299–1313.e19, March 2021.
11. Jun Nagai, Xinzhu Yu, Thomas Papouin, Eunji Cheong, Marc R Freeman, Kelly R Monk, Michael H Hastings, Philip G Haydon, David Rowitch, Shai Shaham, and Baljit S Khakh. Behaviorally consequential astrocytic regulation of neural circuits. *Neuron*, 109(4):576–596, February 2021.

bioRxiv preprint doi: https://doi.org/10.1101/2022.12.29.522099; this version posted December 29, 2022. The copyright holder for this preprint (which was not certified by peer review) is the author/funder, who has granted bioRxiv a license to display the preprint in perpetuity. It is made available under aCC-BY-NC-ND 4.0 International license.

12. Ronald C Kessler, Patricia Berglund, Olga Demler, Robert Jin, Doreen Koretz, Kathleen R Merikangas, A John Rush, Ellen E Walters, Philip S Wang, and National Comorbidity Survey Replication. The epidemiology of major depressive disorder: results from the national comorbidity survey replication (NCS-R). *JAMA*, 289(23):3095–3105, June 2003.

13. Deborah S Hasin, Aaron L Sarvet, Jacquelyn L Meyers, Tulshi D Saha, W June Ruan, Malka Stohl, and Bridget F Grant. Epidemiology of adult DSM-5 major depressive disorder and its specifiers in the united states. *JAMA Psychiatry*, 75(4):336–346, April 2018.

14. Damian F Santomauro, Ana M Mantilla Herrera, Jamileh Shadid, Peng Zheng, Charlie Ashbaugh, David M Pigott, Cristiana Abbafati, Christopher Adolph, Joanne O Amlag, Aleksandr Y Aravkin, Bree L Bang-Jensen, Gregory J Bertolacci, Sabina S Bloom, Rachel Castellano, Emma Castro, Suman Chakrabarti, Jhilik Chattopadhyay, Rebecca M Cogen, James K Collins, Xiaochen Dai, William James Dangel, Carolyn Dapper, Amanda Deen, Megan Erickson, Samuel B Ewald, Abraham D Flaxman, Joseph Jon Frostad, Nancy Fullman, John R Giles, Ababi Zergaw Giref, Gaorui Guo, Jiawei He, Monika Helak, Erin N Hulland, Bulat Idrisov, Akiaja Lindstrom, Emily Linebarger, Paulo A Lotufo, Rafael Lozano, Beatrice Magistro, Deborah Carvalho Malta, Johan C Månsson, Fatima Marinho, Ali H Mokdad, Lorenzo Monasta, Paulami Naik, Shuhei Nomura, James Kevin O'Halloran, Samuel M Ostroff, Maja Pasovic, Louise Penberthy, Robert C Reiner, Jr, Grace Reinke, Antonio Luiz P Ribeiro, Aleksei Sholokhov, Reed J D Sorensen, Elena Varavikova, Anh Truc Vo, Rebecca Walcott, Stefanie Watson, Charles Shey Wiysonge, Bethany Zigler, Simon I Hay, Theo Vos, Christopher J L Murray, Harvey A Whiteford, and Alize J Ferrari. Global prevalence and burden of depressive and anxiety disorders in 204 countries and territories in 2020 due to the COVID-19 pandemic. *Lancet*, 398(10312):1700–1712, November 2021.

15. Pim Cuijpers. The challenges of improving treatments for depression. *JAMA*, 320(24):2529–2530, December 2018.

16. Yu Liu, Deyong Lin, Boliang Wu, and Wenhua Zhou. Ketamine abuse potential and use disorder. *Brain Res. Bull.*, 126(Pt 1):68–73, September 2016.

17. J B Overmier and M E Seligman. Effects of inescapable shock upon subsequent escape and avoidance responding. *J. Comp. Physiol. Psychol.*, 63(1):28–33, February 1967.

18. Aaron S Andalman, Vanessa M Burns, Matthew Lovett-Barron, Michael Broxton, Ben Poole, Samuel J Yang, Logan Grosenick, Talia N Lerner, Ritchie Chen, Tyler Benster, Philippe Mourrain, Marc Levoy, Kanaka Rajan, and Karl Deisseroth. Neuronal dynamics regulating brain and behavioral state transitions. *Cell*, 177(4):970–985.e20, May 2019.

19. American Psychiatric Association. *Diagnostic and Statistical Manual of Mental Disorders*. DSM Library. American Psychiatric Association, May 2013.

20. Melissa R Warden, Aslihan Selimbeyoglu, Julie J Mirzabekov, Maisie Lo, Kimberly R Thompson, Sung-Yon Kim, Avishek Adhikari, Kay M Tye, Loren M Frank, and Karl Deisseroth. A prefrontal cortex-brainstem neuronal projection that controls response to behavioural challenge. *Nature*, 492(7429):428–432, December 2012.

21. Yan Yang, Yihui Cui, Kangning Sang, Yiyan Dong, Zheyi Ni, Shuangshuang Ma, and Hailan Hu. Ketamine blocks bursting in the lateral habenula to rapidly relieve depression. *Nature*, 554(7692):317–322, February 2018.

22. Grazyna Rajkowska and Craig A Stockmeier. Astrocyte pathology in major depressive disorder: insights from human postmortem brain tissue. *Curr. Drug Targets*, 14(11):1225–1236, October 2013.

23. Yihui Cui, Yan Yang, Zheyi Ni, Yiyan Dong, Guohong Cai, Alexandre Foncelle, Shuangshuang Ma, Kangning Sang, Siyang Tang, Yuezhou Li, Ying Shen, Hugues Berry, Shengxi Wu, and Hailan Hu. Astroglial kir4.1 in the lateral habenula drives neuronal bursts in depression. *Nature*, 554(7692):323–327, February 2018.

24. Larissa Grupp, Hartwig Wolburg, and Andreas F Mack. Astroglial structures in the zebrafish brain. *J. Comp. Neurol.*, 518(21):4277–4287, November 2010.

25. Jason Rihel, David A Prober, Anthony Arvanites, Kelvin Lam, Steven Zimmerman, Sumin Jang, Stephen J Haggarty, David Kokel, Lee L Rubin, Randall T Peterson, and Alexander F Schier. Zebrafish behavioral profiling links drugs to biological targets and rest/wake regulation. *Science*, 327(5963):348–351, January 2010.

26. Randall T Peterson, Stanley Y Shaw, Travis A Peterson, David J Milan, Tao P Zhong, Stuart L Schreiber, Calum A MacRae, and Mark C Fishman. Chemical suppression of a genetic mutation in a zebrafish model of aortic coarctation. *Nat. Biotechnol.*, 22(5):595–599, May 2004.

bioRxiv preprint doi: https://doi.org/10.1101/2022.12.29.522099; this version posted December 29, 2022. The copyright holder for this preprint (which was not certified by peer review) is the author/funder, who has granted bioRxiv a license to display the preprint in perpetuity. It is made available under aCC-BY-NC-ND 4.0 International license.

27. Nikita Vladimirov, Yu Mu, Takashi Kawashima, Davis V Bennett, Chao-Tsung Yang, Loren L Looger, Philipp J Keller, Jeremy Freeman, and Misha B Ahrens. Light-sheet functional imaging in fictively behaving zebrafish. *Nat. Methods*, 11(9):883–884, September 2014.

28. Xiuye Chen, Yu Mu, Yu Hu, Aaron T Kuan, Maxim Nikitchenko, Owen Randlett, Alex B Chen, Jeffery P Gavornik, Haim Sompolinsky, Florian Engert, and Misha B Ahrens. Brain-wide organization of neuronal activity and convergent sensorimotor transformations in larval zebrafish. *Neuron*, 100(4):876–890.e5, November 2018.

29. M B Orger, M C Smear, S M Anstis, and H Baier. Perception of fourier and non-fourier motion by larval zebrafish. *Nat. Neurosci.*, 3(11):1128–1133, November 2000.

30. Thomas H McLean, Jason C Parrish, Michael R Braden, Danuta Marona-Lewicka, Alejandra Gallardo-Godoy, and David E Nichols. 1-aminomethylbenzocycloalkanes: conformationally restricted hallucinogenic phenethylamine analogues as functionally selective 5-HT2A receptor agonists. *J. Med. Chem.*, 49(19):5794–5803, September 2006.

31. Meghan Hibicke, Alexus N Landry, Hannah M Kramer, Zoe K Talman, and Charles D Nichols. Psychedelics, but not ketamine, produce persistent antidepressant-like effects in a rodent experimental system for the study of depression. *ACS Chem. Neurosci.*, 11(6):864–871, March 2020.

32. Mario de la Fuente Revenga, Bohan Zhu, Christopher A Guevara, Lynette B Naler, Justin M Saunders, Zirui Zhou, Rudy Toneatti, Salvador Sierra, Jennifer T Wolstenholme, Patrick M Beardsley, George W Huntley, Chang Lu, and Javier González-Maeso. Prolonged epigenomic and synaptic plasticity alterations following single exposure to a psychedelic in mice. *Cell Rep.*, 37(3):109836, October 2021.

33. Lindsay P Cameron, Robert J Tombari, Ju Lu, Alexander J Pell, Zefan Q Hurley, Yann Ehinger, Maxemiliano V Vargas, Matthew N McCarroll, Jack C Taylor, Douglas Myers-Turnbull, Taohui Liu, Bianca Yaghoobi, Lauren J Laskowski, Emilie I Anderson, Guoliang Zhang, Jayashri Viswanathan, Brandon M Brown, Michelle Tjia, Lee E Dunlap, Zachary T Rabow, Oliver Fiehn, Heike Wulff, John D McCorvy, Pamela J Lein, David Kokel, Dorit Ron, Jamie Peters, Yi Zuo, and David E Olson. A non-hallucinogenic psychedelic analogue with therapeutic potential. *Nature*, 589(7842):474–479, January 2021.

34. Anat Levit Kaplan, Danielle N Confair, Kuglae Kim, Ximena Barros-Álvarez, Ramona M Rodriguiz, Ying Yang, Oh Sang Kweon, Tao Che, John D McCorvy, David N Kamber, James P Phelan, Luan Carvalho Martins, Vladimir M Pogorelov, Jeffrey F DiBerto, Samuel T Slocum, Xi-Ping Huang, Jain Manish Kumar, Michael J Robertson, Ouliana Panova, Alpay B Seven, Autumn Q Wetsel, William C Wetsel, John J Irwin, Georgios Skiniotis, Brian K Shoichet, Bryan L Roth, and Jonathan A Ellman. Bespoke library docking for 5-HT2A receptor agonists with antidepressant activity. *Nature*, 610(7932):582–591, October 2022.

35. Chunyang Dong, Calvin Ly, Lee E Dunlap, Maxemiliano V Vargas, Junqing Sun, In-Wook Hwang, Arya Azinfar, Won Chan Oh, William C Wetsel, David E Olson, and Lin Tian. Psychedelic-inspired drug discovery using an engineered biosensor. *Cell*, 184(10):2779–2792.e18, May 2021.

36. Jordi Bonaventura, Juan L Gomez, Meghan L Carlton, Sherry Lam, Marta Sanchez-Soto, Patrick J Morris, Ruin Moaddel, Hye Jin Kang, Panos Zanos, Todd D Gould, Craig J Thomas, David R Sibley, Carlos A Zarate, Jr, and Michael Michaelides. Target deconvolution studies of (2R,6R)-hydroxynorketamine: an elusive search. *Mol. Psychiatry*, June 2022.

37. R Trullas and P Skolnick. Functional antagonists at the NMDA receptor complex exhibit antidepressant actions. *Eur. J. Pharmacol.*, 185(1):1–10, August 1990.

38. Erinn S Gideons, Ege T Kavalali, and Lisa M Monteggia. Mechanisms underlying differential effectiveness of memantine and ketamine in rapid antidepressant responses. *Proc. Natl. Acad. Sci. U. S. A.*, 111(23):8649–8654, June 2014.

39. Calvin Ly, Alexandra C Greb, Lindsay P Cameron, Jonathan M Wong, Eden V Barragan, Paige C Wilson, Kyle F Burbach, Sina Soltanzadeh Zarandi, Alexander Sood, Michael R Paddy, Whitney C Duim, Megan Y Dennis, A Kimberley McAllister, Kassandra M Ori-McKenney, John A Gray, and David E Olson. Psychedelics promote structural and functional neural plasticity. *Cell Rep.*, 23(11):3170–3182, June 2018.

40. Nanxin Li, Boyoung Lee, Rong-Jian Liu, Mounira Banasr, Jason M Dwyer, Masaaki Iwata, Xiao-Yuan Li, George Aghajanian, and Ronald S Duman. mTOR-dependent synapse formation underlies the rapid antidepressant effects of NMDA antagonists. *Science*, 329(5994):959–964, August 2010.

bioRxiv preprint doi: https://doi.org/10.1101/2022.12.29.522099; this version posted December 29, 2022. The copyright holder for this preprint (which was not certified by peer review) is the author/funder, who has granted bioRxiv a license to display the preprint in perpetuity. It is made available under aCC-BY-NC-ND 4.0 International license.

41. Akira Kudoh, Yoko Takahira, Hiroshi Katagai, and Tomoko Takazawa. Small-dose ketamine improves the postoperative state of depressed patients. *Anesth. Analg.*, 95(1):114–8, table of contents, July 2002.

42. Shijia Chen, Cindy N Chiu, Kimberly L McArthur, Joseph R Fetcho, and David A Prober. TRP channel mediated neuronal activation and ablation in freely behaving zebrafish. *Nat. Methods*, 13(2):147–150, February 2016.

43. Hiromu Monai, Masamichi Ohkura, Mika Tanaka, Yuki Oe, Ayumu Konno, Hirokazu Hirai, Katsuhiko Mikoshiba, Shigeyoshi Itohara, Junichi Nakai, Youichi Iwai, and Hajime Hirase. Calcium imaging reveals glial involvement in transcranial direct current stimulation-induced plasticity in mouse brain. *Nat. Commun.*, 7:11100, March 2016.

44. Kuglae Kim, Tao Che, Ouliana Panova, Jeffrey F DiBerto, Jiankun Lyu, Brian E Krumm, Daniel Wacker, Michael J Robertson, Alpay B Seven, David E Nichols, Brian K Shoichet, Georgios Skiniotis, and Bryan L Roth. Structure of a Hallucinogen-Activated Gq-Coupled 5-HT2A serotonin receptor. *Cell*, 182(6):1574–1588.e19, September 2020.

45. Youyi Zhang, Fei Ye, Tongtong Zhang, Shiyun Lv, Liping Zhou, Daohai Du, He Lin, Fei Guo, Cheng Luo, and Shujia Zhu. Structural basis of ketamine action on human NMDA receptors. *Nature*, 596(7871):301–305, August 2021.

46. Jessica Burgstaller, Elena Hindinger, Joseph Donovan, Marco Dal Maschio, Andreas M Kist, Benno Gesierich, Ruben Portugues, and Herwig Baier. Light-sheet imaging and graph analysis of antidepressant action in the larval zebrafish brain network. July 2019.

47. Brooke Short, Joanna Fong, Veronica Galvez, William Shelker, and Colleen K Loo. Side-effects associated with ketamine use in depression: a systematic review. *Lancet Psychiatry*, 5(1):65–78, January 2018.

48. Vincenzo Oliva, Matteo Lippi, Riccardo Paci, Lorenzo Del Fabro, Giuseppe Delvecchio, Paolo Brambilla, Diana De Ronchi, Giuseppe Fanelli, and Alessandro Serretti. Gastrointestinal side effects associated with antidepressant treatments in patients with major depressive disorder: A systematic review and meta-analysis. *Prog. Neuropsychopharmacol. Biol. Psychiatry*, 109:110266, July 2021.

49. Hod Dana, Boaz Mohar, Yi Sun, Sujatha Narayan, Andrew Gordus, Jeremy P Hasseman, Getahun Tsegaye, Graham T Holt, Amy Hu, Deepika Walpita, Ronak Patel, John J Macklin, Cornelia I Bargmann, Misha B Ahrens, Eric R Schreiter, Vivek Jayaraman, Loren L Looger, Karel Svoboda, and Douglas S Kim. Sensitive red protein calcium indicators for imaging neural activity. *Elife*, 5, March 2016.

50. Timothy W Dunn, Yu Mu, Sujatha Narayan, Owen Randlett, Eva A Naumann, Chao-Tsung Yang, Alexander F Schier, Jeremy Freeman, Florian Engert, and Misha B Ahrens. Brain-wide mapping of neural activity controlling zebrafish exploratory locomotion. *Elife*, 5:e12741, March 2016.

51. Paride Antinucci, Adna Dumitrescu, Charlotte Deleuze, Holly J Morley, Kristie Leung, Tom Hagley, Fumi Kubo, Herwig Baier, Isaac H Bianco, and Claire Wyart. A calibrated optogenetic toolbox of stable zebrafish opsin lines. *Elife*, 9, March 2020.

52. Richard Mark White, Anna Sessa, Christopher Burke, Teresa Bowman, Jocelyn LeBlanc, Craig Ceol, Caitlin Bourque, Michael Dovey, Wolfram Goessling, Caroline Erter Burns, and Leonard I Zon. Transparent adult zebrafish as a tool for in vivo transplantation analysis. *Cell Stem Cell*, 2(2):183–189, February 2008.

53. Akihiro Urasaki, Kazuhide Asakawa, and Koichi Kawakami. Efficient transposition of the tol2 transposable element from a single-copy donor in zebrafish. *Proc. Natl. Acad. Sci. U. S. A.*, 105(50):19827–19832, December 2008.

54. Armin Bahl and Florian Engert. Neural circuits for evidence accumulation and decision making in larval zebrafish. *Nat. Neurosci.*, 23(1):94–102, January 2020.

55. Nathan C Klapoetke, Yasunobu Murata, Sung Soo Kim, Stefan R Pulver, Amanda Birdsey-Benson, Yong Ku Cho, Tania K Morimoto, Amy S Chuong, Eric J Carpenter, Zhijian Tian, Jun Wang, Yinlong Xie, Zhixiang Yan, Yong Zhang, Brian Y Chow, Barbara Surek, Michael Melkonian, Vivek Jayaraman, Martha Constantine-Paton, Gane Ka-Shu Wong, and Edward S Boyden. Independent optical excitation of distinct neural populations. *Nat. Methods*, 11(3):338–346, March 2014.

bioRxiv preprint doi: https://doi.org/10.1101/2022.12.29.522099; this version posted December 29, 2022. The copyright holder for this preprint (which was not certified by peer review) is the author/funder, who has granted bioRxiv a license to display the preprint in perpetuity. It is made available under aCC-BY-NC-ND 4.0 International license.

Supplementary Materials

Supplementary Discussion

Ketamine does not affect baseline locomotion or optomotor response. Related to Figure 1. Because ketamine treatment may have lasting effects on larval zebrafish's swimming in baseline conditions, we performed several analyses and experiments to verify that ketamine's suppressive effects on futility-induced passivity were not due to systemic changes in baseline fish behavior that persisted after 1h recovery. First, we compared swim vigor and frequency during closed-loop between ketamine-treated and control fish and found that ketamine-treated fish did not differ significantly from controls in either swim frequency or vigor (Extended Data Fig. 1a-b). As a further test of whether ketamine treatment affects baseline swim drive following washout, we tracked freely swimming fish treated with ketamine or same-clutch controls treated with vehicle as they swam freely in circular arenas with a bottom-projected, non-directional random dot stimulus. We found that freely swimming control and ketamine-treated fish exhibit no difference in swim rate after recovery (Extended Data Fig. 1c). Therefore, ketamine appears to have little effect on either baseline swimming or swimming evoked by closed-loop forward gratings. Furthermore, ketamine seems not to affect motion vision in larval zebrafish due to the similarity in stimulus-evoked swimming.

Addressing potential confounding factors for ketamine's passivity-suppressing effect. Related to Figure 1. We sought to rule out several trivial explanations for ketamine's suppressive effects on passivity during the open-loop conditions. First, ketamine might prevent the fish from distinguishing the open-loop from closed-loop conditions by decreasing the fish's ability to detect changes in its sensorimotor gain. To address this possibility, we analyzed the fish's swimming behavior during open-loop. We found that during open-loop, in response to a decrease in sensorimotor gain, fish swam with higher vigor (Extended Data Fig. 1e), demonstrating intact gain adaptation. Moreover, fish still struggled during open-loop (Fig. 1d), suggesting that futility-induced struggling remained intact.

Second, ketamine acts as an anesthetic in many animals, including larval zebrafish. Ketamine's passivity-suppressing effects in open-loop might be due to a rebound effect following recovery from anesthesia. We reasoned that this is unlikely due to a lack of change in swimming behavior in either free-swimming or head-embedded closed loop conditions (Extended Data Fig. 1). However, we also directly tested this possibility by treating fish with MS-222, a sodium channel blocker used as an anesthetic in zebrafish but with no known anxiolytic or antidepressant effects. We treated fish in MS-222 for one hour and, following recovery, tested the fish or same-clutch controls treated with the vehicle in tail-free giving up. As expected, both MS-222 and ketamine act as an anesthetic in fish and suppress swimming at the concentrations tested (Extended Data Fig. 2a-b). However, we found that, in contrast to ketamine-treated fish, fish treated with MS-222 exhibited no decrease in passivity during open loop compared to controls (Extended Data Fig. 2c). Therefore, the passivity-suppressing effects of ketamine during open loop are likely not a consequence of its anesthetic effects.

bioRxiv preprint doi: https://doi.org/10.1101/2022.12.29.522099; this version posted December 29, 2022. The copyright holder for this preprint (which was not certified by peer review) is the author/funder, who has granted bioRxiv a license to display the preprint in perpetuity. It is made available under aCC-BY-NC-ND 4.0 International license.

Extended Data

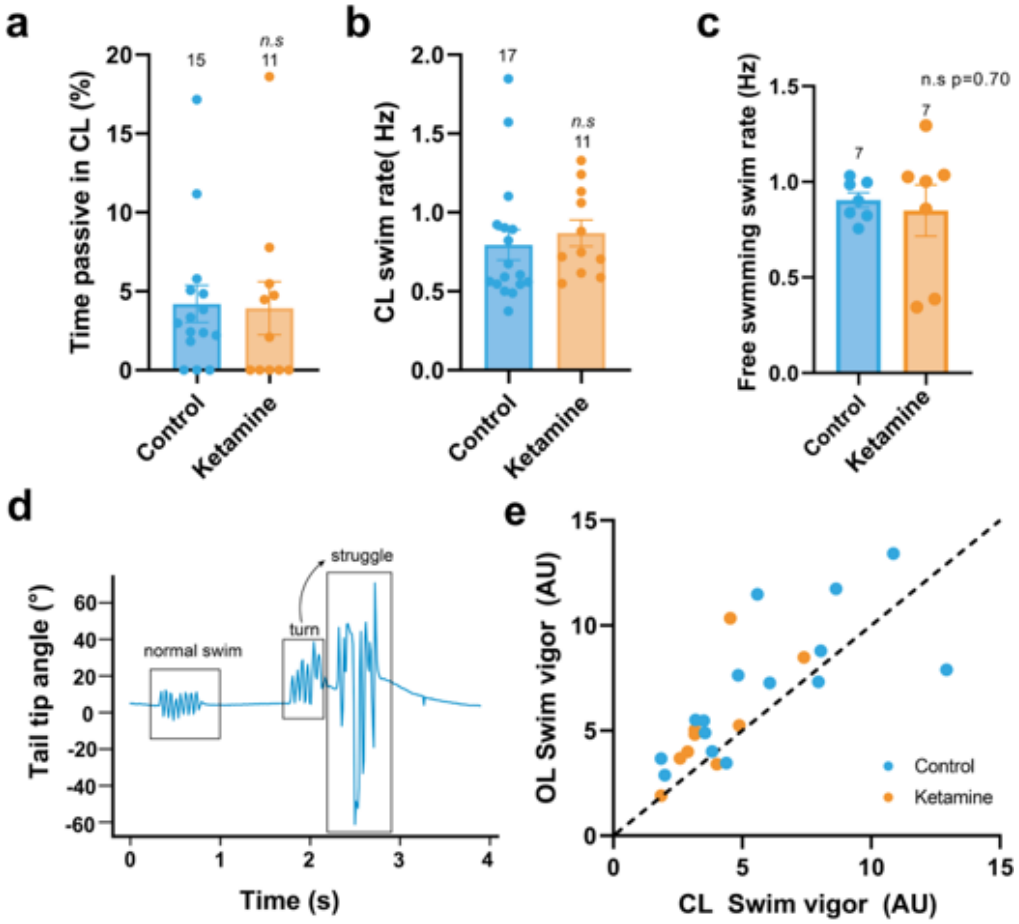

Extended Data Figure 1. Additional closed-loop and open-loop swimming statistics in ketamine-treated and control fish. (a) Average percentage of CL interval spent in the passive state. Individual dots represent trial averages for each fish. Control and ketamine fish exhibit similar average % passive time in CL (t-test, $p = 0.8921$). (b) A comparison of closed-loop (CL) swim rate in control and ketamine-treated fish. Individual dots represent trial averages for each fish. Control and ketamine fish exhibit similar average swim rate (t-test, $p = 0.5898$). (c) A comparison of closed-loop (CL) swim rate in control and ketamine-treated fish. Individual dots represent trial averages for each fish. Control and ketamine fish exhibit similar average swim rate (t-test, $p = 0.70$). (d) Example snippet showing the angle made by the tip of the tail relative to the fish's long body axis during a 4 s period during open-loop swimming. Three different bout types, a representative normal swim, turn (asymmetric tail angle) and struggle (large amplitude, uncoordinated swimming), can be seen and are manually annotated. The observed turn transitions into a struggle with little inter-swim interval, denoted by the arrow. (e) Average swim vigor (peak value of detected swim bouts yielded by 500 ms moving standard deviation (see Methods) during open loop plotted against average swim vigor during closed loop. Each point represents the trial average of an individual fish. While the OL to CL ratio does not differ between control and ketamine-treated fish (t-test on slope, $p = 0.7097$), both control and ketamine-treated fish exhibited more vigorous swimming in OL than in CL (paired t-test mean vigor OL-CL > 0 $p = 0.0268$ for ketamine, $p = 0.0347$ for control). All error bars represent s.e.m.

bioRxiv preprint doi: https://doi.org/10.1101/2022.12.29.522099; this version posted December 29, 2022. The copyright holder for this preprint (which was not certified by peer review) is the author/funder, who has granted bioRxiv a license to display the preprint in perpetuity. It is made available under aCC-BY-NC-ND 4.0 International license.

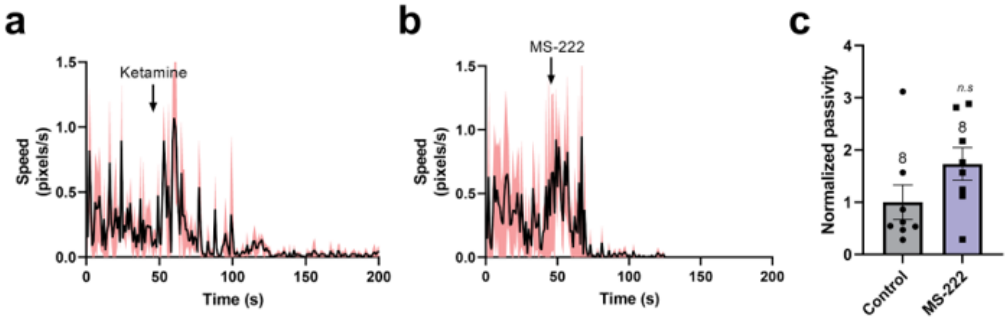

Extended Data Figure 2. The anesthetic tricaine (MS-222) does not decrease open-loop passivity following 1 h recovery, but anesthetizes the fish and blocks neuronal activity. (a-b) Comparison of ketamine and tricaine's anesthetic effects. Traces represent mean and s.e.m of swim rate across fish following application of either (a) ketamine or (b) tricaine (MS-222). (c) Average percentage of open-loop (OL) interval spent passive in fish treated with tricaine for 1 h and allowed to recover for 1 h versus fish treated with vehicle control. There is no significant reduction in passivity during the OL period in tricaine-treated fish relative to control (two-tailed t-test, $p = 0.1301$, $n = 8$).

bioRxiv preprint doi: https://doi.org/10.1101/2022.12.29.522099; this version posted December 29, 2022. The copyright holder for this preprint (which was not certified by peer review) is the author/funder, who has granted bioRxiv a license to display the preprint in perpetuity. It is made available under aCC-BY-NC-ND 4.0 International license.

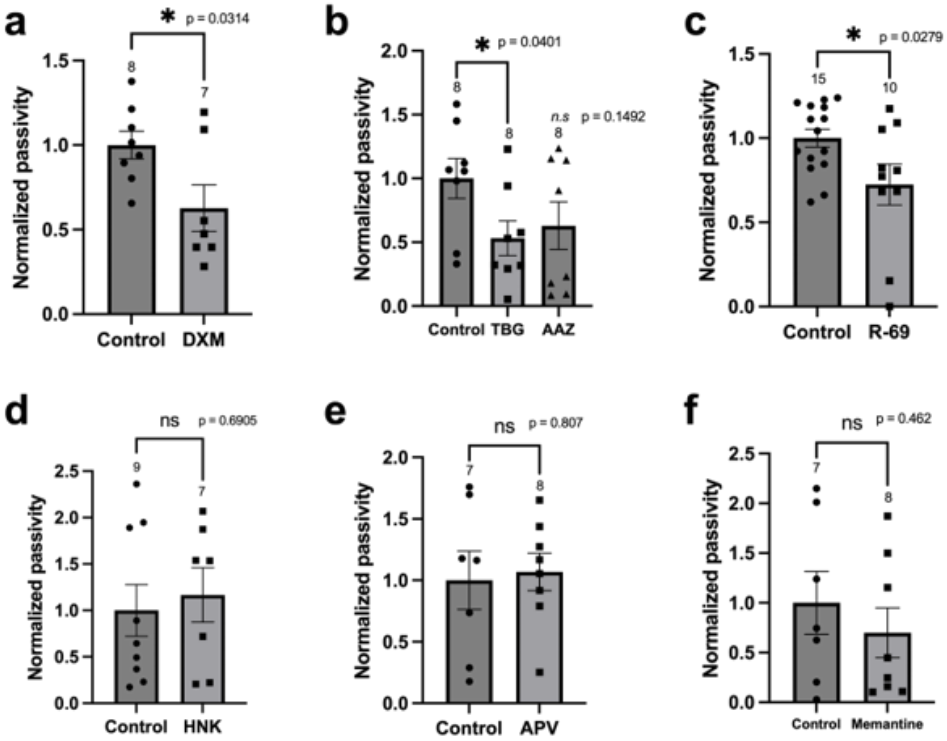

Extended Data Figure 3. Additional compounds tested in our assay. (**a-f**) Effect on passivity in the zFST test after treatment with compounds shown in Figure 2A compared to their same clutch controls. All error bars represent s.e.m. Two-tailed t-test with p-value indicated in each plot and number of fish above each bar.

bioRxiv preprint doi: https://doi.org/10.1101/2022.12.29.522099; this version posted December 29, 2022. The copyright holder for this preprint (which was not certified by peer review) is the author/funder, who has granted bioRxiv a license to display the preprint in perpetuity. It is made available under aCC-BY-NC-ND 4.0 International license.

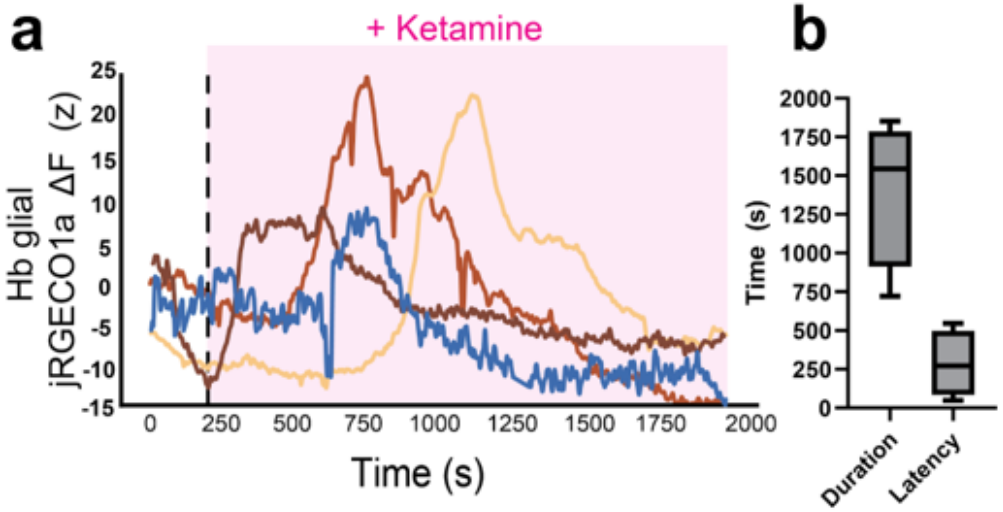

Extended Data Figure 4. Astroglial calcium imaging during ketamine treatment: individual fish results and summary statistics. (a) Mean astroglial fluorescence from hindbrain ROI for jRGECO in different fish after ketamine treatment. (b) Amplitude and latency (time to peak after ketamine administration) of the astrocytic calcium wave induced by ketamine (n = 4 fish). Mean±SEM Amplitude = 1414s ±242.9. Latency = 285.4s ±105.7.

bioRxiv preprint doi: https://doi.org/10.1101/2022.12.29.522099; this version posted December 29, 2022. The copyright holder for this preprint (which was not certified by peer review) is the author/funder, who has granted bioRxiv a license to display the preprint in perpetuity. It is made available under aCC-BY-NC-ND 4.0 International license.

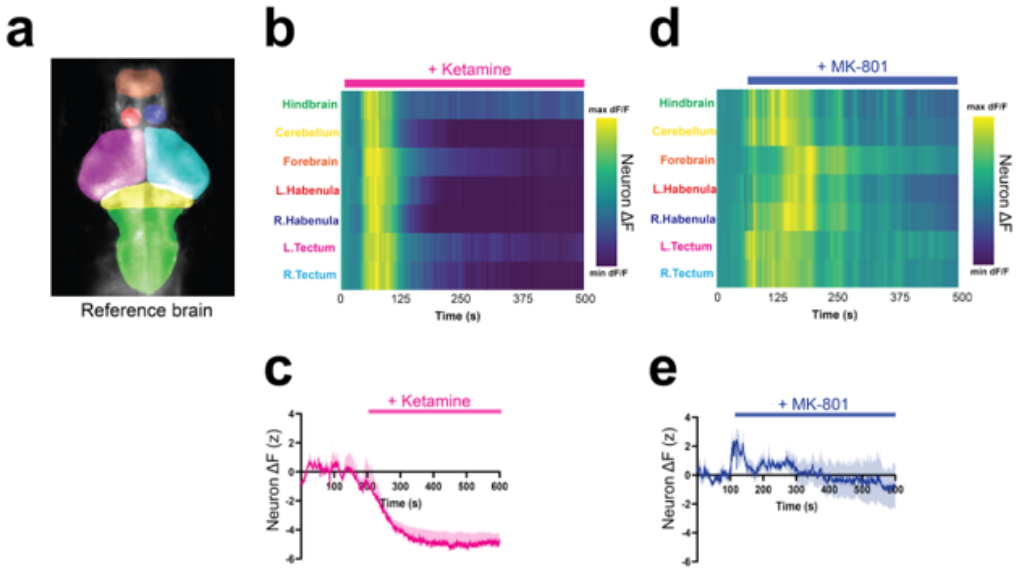

Extended Data Figure 5. Additional data on MK-801 and ketamine effects on neuronal activity and behavior. (a)Transgenic fish expressing the nuclear calcium indicator H2B-GCaMP7f in neurons using the elavl3 promoter were imaged using an epifluorescence microscope. Panel shows seven regions of interest (different colors) across the brain where we measured activity. (b) Example heatmaps showing dF/F for each region of interest after treatment with ketamine. Pink bar above heatmap denotes time when ketamine is in bath. (c) Mean fluorescence across all ROIs (n = 4 fish) after treatment with ketamine. (d) Example heatmaps showing dF/F for each region of interest after treatment with MK-801. Blue bar above heatmap denotes time when MK-801 is in bath. (e) Mean fluorescence across all ROIs (n = 4 fish) after treatment with MK-801.

bioRxiv preprint doi: https://doi.org/10.1101/2022.12.29.522099; this version posted December 29, 2022. The copyright holder for this preprint (which was not certified by peer review) is the author/funder, who has granted bioRxiv a license to display the preprint in perpetuity. It is made available under aCC-BY-NC-ND 4.0 International license.

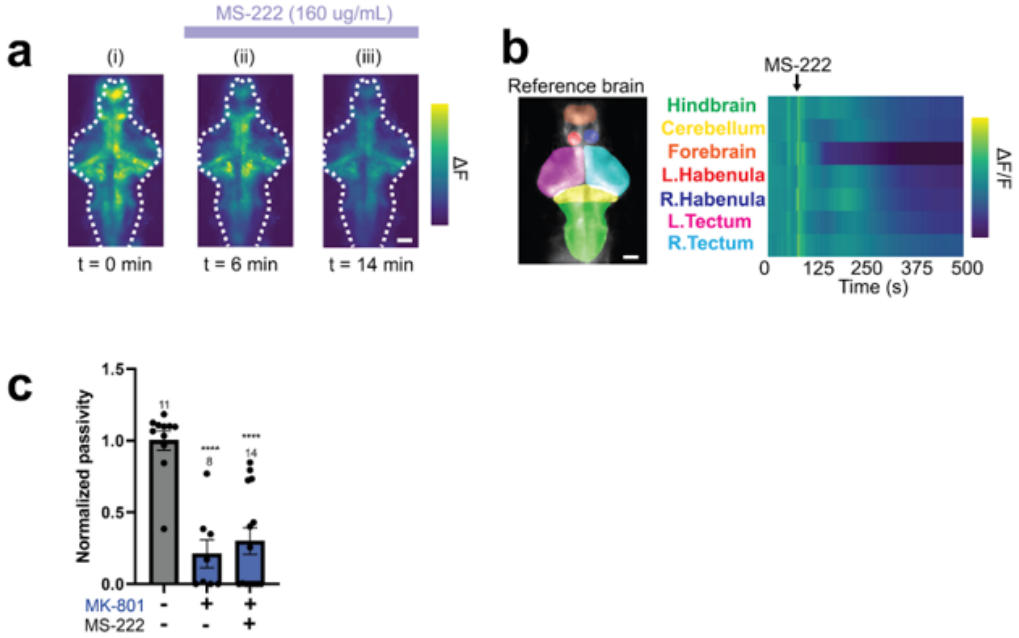

Extended Data Figure 6. Effects of MS-222 on neural activity and behavior. (a) Fluorescence micrograph images in an example H2B-GCaMPf7 fish (i) immediately prior to MS-222 addition at t = 0 min, (ii) at t = 6 min and (iii) at t = 14 min when cytosolic calcium has decreased in most brain areas. Purple bar denotes times when MS-222 is in the bath. (b) Time course of neuronal H2B-GCaMP7f signal in seven regions of interest (different colors, left). MS-222 addition indicated by arrow and evident from small fluorescence artifact. Note decrease of activity in most brain areas by 300s, specially in the forebrain. (c) Open-loop passivity in zFST for fish treated with MK-801, with or without neural activity blocker MS-222. MK-801, similar to ketamine, still suppresses passivity in the presence of MS-222. **** p¡0.0001 with two-tailed t-test with Bonferroni correction. Control group is shared with Fig. 3G and so is repeated here. (b-c) Scale bar 50 μm.

bioRxiv preprint doi: https://doi.org/10.1101/2022.12.29.522099; this version posted December 29, 2022. The copyright holder for this preprint (which was not certified by peer review) is the author/funder, who has granted bioRxiv a license to display the preprint in perpetuity. It is made available under aCC-BY-NC-ND 4.0 International license.

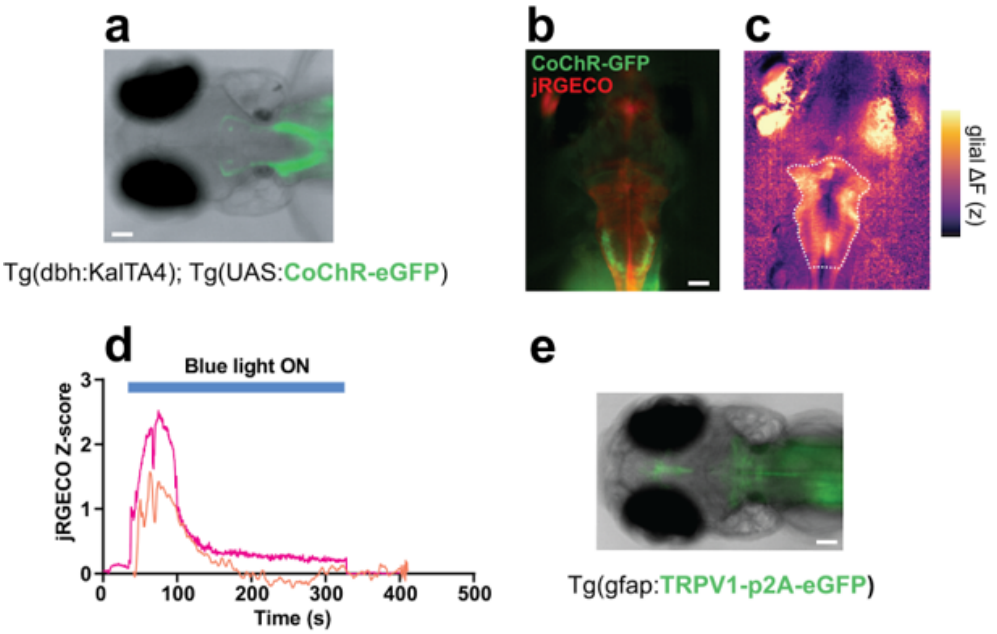

Extended Data Figure 7. Supplementary information regarding optogenetic and chemogenetic experiments. (a) Overlaid fluorescence and transmitted light image of a larval zebrafish expressing eGFP-fused CoChR (a channelrhodopsin) under the dbh promoter, Expression in noradrenergic neurons evidence from fluorescence in anatomically distinct axon tracts. (b) Overlaid red- and green-channel fluorescence images showing double transgenic fish lines used for simultaneous imaging of glial cytosolic calcium and stimulating NE neurons. Fish express eGFP-fused CoChR under the dbh promoter and the red calcium indicator jRGECO1a under the gfap promoter. (c) Imaging frame taken during blue-light (488 nm) stimulation of NE neurons while imaging astroglial cytosolic Ca. (d) Time-course of jRGECO1a signal in two different fish during blue-light stimulations. (e) Overlaid fluorescence and transmitted light image of a larval zebrafish expressing GFP-fused rat TRPV1 in astroglia under the gfap promoter. Scale bars 50 μm.

bioRxiv preprint doi: https://doi.org/10.1101/2022.12.29.522099; this version posted December 29, 2022. The copyright holder for this preprint (which was not certified by peer review) is the author/funder, who has granted bioRxiv a license to display the preprint in perpetuity. It is made available under aCC-BY-NC-ND 4.0 International license.

Extended Data Table 1. List, sources, and concentrations of compounds used in pharmacological experiments.

Compound	Vehicle	Stock conc.	Final conc.	Reference	Source
MS-222 (Tricaine)	water	160 mg/mL	160 μg/mL	[1]	Sigma E10521
Ketamine HCl	water	100 mg/mL	0.8 mM	[2]	Patterson Veterinary xE07-803-6637
Dextromethorphan (DXM)	water	50 mM	50 μM	[3]	Sigma D9684
AP-5	water	50 mM	0.5 mM	[4]	Sigma A8054
MK-801 maleate	water	40 mM	40 μM	[5]	Cayman Chemicals 10009019
Fluoxetine HCl	water	5 mM	5 μM	[2]	Sigma F132
Escitalopram oxalate	water	10 mM	10 μM	[6]	Sigma E4786
Desipramine HCl	water	50 mM	50 μM	[7]	Sigma D3900
TCB-2	DMSO	50 mM	50 μM	[8]*	Cayman Chemicals 2592
R69 HCl	water	70 mM	0.7 mM	[9]*	Roth Lab
TBG fumarate	water	10 mM	0.1 mM	[9,10]*	Olson Lab
AAZ HCl	water	70 mM	0.7 mM	[9]*	Olson Lab
Memantine HCl	water	50 mM	50 μM	[4]	Sigma M9292
DOI HCl (+/-)	water	30 mM	0.3 mM	[9]*	Sigma D101
(R,R)-HNK	water	70 mM	0.7 mM	[9]*	Sigma SML1873

[1] Same concentration used in C. Leyden *et al. Front Vet Sci.* 9, 864573 (2022).
[2] Same concentration used in A. S. Andalman *et al. Cell.* 177, 970–985.e20 (2019).
[3] Same concentration used in Z. Xu *et al. J. Appl. Toxicol.* 31, 157–163 (2011).
[4] J. D. Best *et al. Neuropsychopharmacology.* 33, 1206–1215 (2008). Range used more similar to ketamine for fair comparison.
[5] Same concentration used in J. Chen *et al. Int. J. Comp. Psychol.* 23, 82–90 (2010).
[6] Same as fluoxetine but used higher concentration due to decreased toxicity.
[7] Same concentration used in J. Cueto-Escobedo *et al. Front. Behav. Neurosci.* 15, 795285 (2021).
[8] Tested different concentrations.
[9] Matching ketamine's concentration range.
[10] Safety in larval zebrafish assessed assessed at 0.1mM in L. P. Cameron *et al. Nature.* 589, 474–479 (2021).
* no record of testing in larval zebrafish

bioRxiv preprint doi: https://doi.org/10.1101/2022.12.29.522099; this version posted December 29, 2022. The copyright holder for this preprint (which was not certified by peer review) is the author/funder, who has granted bioRxiv a license to display the preprint in perpetuity. It is made available under aCC-BY-NC-ND 4.0 International license.

Extended Data Table 2. Statistical tests, sample sizes, and p values reported for all relevant panels of Figures 1-4.

Panel	**Test**	**n (num. fish)**	p
Fig. 1e	Two-tailed t-test	16 (control), 15 (ketamine)	0.0045
Fig. 1f	Two-tailed t-test	8 (control), 8 (ketamine)	0.0242
Fig. 2b	One-way ANOVA with Tukey's multiple comparison test (vs. control)	17 (control), 10 (ketamine), 8 (MK-801)	0.0086 (ketamine), 0.0115 (MK8-801)
Fig. 2c	One-way ANOVA with Tukey's multiple comparison test (vs. control)	24 (control), 8 (fluoxetine), 8 (citalopram), 8 desipramine	0.4790 (fluoxetine), 0.9990 (citalopram), 0.0036 (desipramine)
Fig. 2d	One-way ANOVA with Tukey's multiple comparison test (vs. control)	16 (control), 8 (DOI), 7 (TCB-2)	$<$ 0.0001 (DOI), 0.0008 (TCB-2)
Fig. 2e	One-way ANOVA with Tukey's multiple comparison test (vs. control)	8 (control), 8 (ketamine), 8 (MK-801)	0.0103 (ketamine), $<$ 0.0001 (MK-801)
Fig. 2f	One-way ANOVA with Tukey's multiple comparison test (vs. control)	8 (control), 8 (fluoxetine), 8 (desipramine)	0.2392 (fluoxetine), 0.0017 (desipramine)
Fig. 2g	One-way ANOVA with Tukey's multiple comparison test (vs. control)	16 (control), 8 (DOI), 8 (TCB-2)	0.8096 (DOI), 0.8295 (TCB-2)
Fig. 3e	One-way ANOVA with Tukey's multiple comparison test (vs. control)	5 (control, MS-222), 5 (MS-222), 4 (all other conditions)	0.0149 (MK801), 0.0169 (Ketamine), 0.9395 (Tricaine), 0.9893 (DOI), 0.9996 (Fluoxetine)
Fig. 3g	Two-way ANOVA with Tukey's multiple comparison test (vs. control)	11 (control), 10 (ketamine), 12 (ketamine + MS-222), 8 (tricaine)	No interaction (0.1948) 0.6990 (ket vs ket + MS-222), 0.0003 MS-222 vs ketamine + MS-222)
Fig. 3h	Two-way ANOVA with Tukey's multiple comparison test (vs. control)	5 (control and MS-222), 4 (all other conditions)	No interaction (0.9541), 0.6990 (control vs MS-222), 0.6761 (ketamine. vs ketamine+ MS-222), 0.0004 (control vs ketamine + MS-222)

cont. next page.

bioRxiv preprint doi: https://doi.org/10.1101/2022.12.29.522099; this version posted December 29, 2022. The copyright holder for this preprint (which was not certified by peer review) is the author/funder, who has granted bioRxiv a license to display the preprint in perpetuity. It is made available under aCC-BY-NC-ND 4.0 International license.

Extended Data Table 2 (Cont.)

Panel	**Test**	**n (num. fish)**	p
Fig. 4b	Two-tailed t-test	15 (dbh:CoChr, no light), 6 (wild type, blue light), 13 (dbh:CoChr, blue light)	0.0197 (WT-Blue light vs DBH-Blue light)
Fig. 4e	Two-tailed t-test	14 (Control), 12 (Capsaicin)	0.0229
Fig. 4g,i	-	4 (Pre), 4 (Post)	-
Fig. 4j	Two-tailed t-test	4 (Pre), 4 (Post), 7 swims analyzed for each group	0.0056

bioRxiv preprint doi: https://doi.org/10.1101/2022.12.29.522099; this version posted December 29, 2022. The copyright holder for this preprint (which was not certified by peer review) is the author/funder, who has granted bioRxiv a license to display the preprint in perpetuity. It is made available under aCC-BY-NC-ND 4.0 International license.

Supplementary Video 1. Example video of a control 7dpf larval zebrafish in the zFST. Example 10 s in rest (no forward drift, feedback), followed by 10s in closed loop (forward drift, feedback) and 10s in open loop (forward drift, no feedback). The 3 intervals are discontinuous and have been merged for visualization purposes.

Supplementary Video 2. Example video of a 7 dpf larval ketamine-treated larval zebrafish in the zFST following recovery from the acute effects of ketamine treatment. Example 10s in rest (no forward drift, feedback), followed by 10 s in closed loop (forward drift, feedback) and 10 s in open loop (forward drift, no feedback). The 3 intervals are discontinuous and have been merged for visualization purposes.

Supplementary Video 3. Example video of an astroglial calcium wave in response to acute ketamine treatment. ΔF of whole-brain jRGECO1a signal expressed under the *gfap* promoter imaged with an epifluorescence scope at 2 Hz. Ketamine was introduced to the water bath after 5 minutes. Scale bar 50 μm.